

## Solution, structural and photophysical aspects of substituent effects in the N<sup>^</sup>N ligand in [Ir(C<sup>^</sup>N)<sub>2</sub>(N<sup>^</sup>N)]<sup>+</sup> complexes†

Cite this: *Dalton Trans.*, 2013, **42**, 8086

Edwin C. Constable,<sup>a</sup> Catherine E. Housecroft,<sup>\*a</sup> Peter Kopecky,<sup>a</sup> Colin J. Martin,<sup>a</sup> Iain A. Wright,<sup>a</sup> Jennifer A. Zampese,<sup>a</sup> Henk J. Bolink<sup>b</sup> and Antonio Pertegas<sup>b</sup>

The syntheses and properties of a series of eleven new [Ir(ppy)<sub>2</sub>(N<sup>^</sup>N)]PF<sub>6</sub> complexes (Hppy = 2-phenylpyridine) are reported. The N<sup>^</sup>N ligands are based on 2,2'-bipyridine (bpy), substituted in the 6- or 5-positions with groups that are structurally and electronically diverse. All but two of the N<sup>^</sup>N ligands incorporate an aromatic ring, designed to facilitate intra-cation face-to-face π-interactions between the N<sup>^</sup>N and one [ppy]<sup>-</sup> ligand. Within the set of ligands, 6-(3-tolyl)-2,2'-bipyridine (**5**), 4,6-bis(4-nitrophenyl)-2,2'-bipyridine (**9**), and 4,6-bis(3,4,5-trimethoxyphenyl)-2,2'-bipyridine (**10**) are new and their characterization includes single crystal structures of **9**, and two polymorphs of **10**. A representative [Ir(ppy)<sub>2</sub>(N<sup>^</sup>O)]<sup>+</sup> complex is also described. We report solution NMR spectroscopic, photophysical and electrochemical properties of the complexes, as well as representative solid-state structural data. The solution <sup>1</sup>H NMR spectroscopic data illustrate different dynamic processes involving the substituents attached to the bpy domain in the ligands. In degassed MeCN and at room temperature, the [Ir(ppy)<sub>2</sub>(N<sup>^</sup>N)]PF<sub>6</sub> complexes are orange emitters with λ<sub>max</sub><sup>em</sup> in the range 575 to 608 nm; however, quantum yields are very low. The most promising complexes were evaluated in light-emitting electrochemical cells leading to bright and stable devices with rather good external quantum efficiencies.

Received 22nd February 2013,  
Accepted 1st April 2013

DOI: 10.1039/c3dt50492a

www.rsc.org/dalton

### Introduction

Solid-state light-emitting electrochemical cells (LECs) which incorporate octahedral iridium(III) complexes [Ir(C<sup>^</sup>N)<sub>2</sub>(N<sup>^</sup>N)]<sup>+</sup> (C<sup>^</sup>N = a cyclometallated ligand, and N<sup>^</sup>N = 2,2'-bipyridine (bpy), 1,10-phenanthroline or related chelating ligand) in the emissive layer<sup>1</sup> are currently the focus of considerable attention.<sup>2–5</sup> Manipulation of the electronic properties of the ligands by judicious choice of functionalities can lead to enhanced emission and tuning of the emission energy.<sup>6–9</sup> An interplay of experimental and computational results is proving to be an important approach to the development of [Ir(C<sup>^</sup>N)<sub>2</sub>(N<sup>^</sup>N)]<sup>+</sup> emitters.<sup>10</sup> Incorporation of a pendant phenyl ring adjacent to one N-donor of the N<sup>^</sup>N ligand results in intra-cation face-to-face π-stacking with one of the coordinated C<sup>^</sup>N ligands, and this structural feature has a strong influence

on the photophysical properties of the complex<sup>11</sup> and improves LEC device lifetimes.<sup>12–17</sup>

In this paper, we describe the preparation and properties of a series of eleven new [Ir(ppy)<sub>2</sub>(N<sup>^</sup>N)]<sup>+</sup> complexes (Hppy = 2-phenylpyridine) in which the N<sup>^</sup>N ligands **1–11** (Scheme 1) have been selected to encompass a range of electron-withdrawing and electron-releasing substituents. A representative [Ir(ppy)<sub>2</sub>(N<sup>^</sup>O)]<sup>+</sup> complex (N<sup>^</sup>O = **12**, Scheme 1) is also described. We report their solution NMR spectroscopic, photophysical and electrochemical properties as well as representative solid-state structural data.

### Experimental

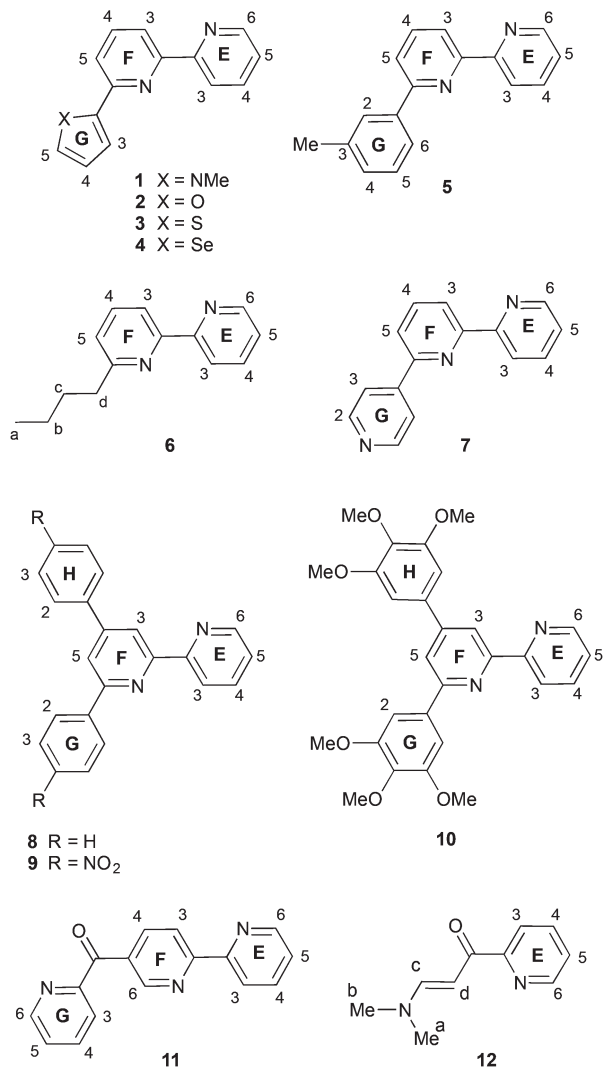
#### General

Bruker Avance III-500 or Avance III-600 NMR spectrometers were used to record <sup>1</sup>H and <sup>13</sup>C NMR spectra; chemical shifts were referenced to residual solvent peaks with respect to δ(TMS) = 0 ppm. Solution electronic absorption and emission spectra were recorded on an Agilent 8453 spectrophotometer and Shimadzu RF-5301 PC spectrofluorometer, respectively, and FT-IR spectra on a Shimadzu 8400S instrument with Golden Gate accessory for solid samples. Quantum yields were

<sup>a</sup>Department of Chemistry, University of Basel, Spitalstrasse 51, CH-4056 Basel, Switzerland. E-mail: catherine.housecroft@unibas.ch

<sup>b</sup>Instituto de Ciencia Molecular, Universidad de Valencia, C/Catedrático J. Beltrán 2, ES-46980 Paterna (Valencia), Spain

†CCDC 910293, 910295, 910297, 925640–925643. For crystallographic data in CIF or other electronic format see DOI: 10.1039/c3dt50492a



**Scheme 1** Structures of ligands **1–12** and numbering schemes for NMR spectroscopic assignments.

measured with an absolute PL quantum yield spectrometer C11347 Quantaury\_QY from Hamamatsu. Thin film photoluminescence spectra and quantum yields were measured with a Hamamatsu C9920-02 Absolute PL Quantum Yield Measurement System ( $\lambda_{\text{exc}} = 314 \text{ nm}$ ). The system is made up of an excitation light source, consisting of a xenon lamp linked to a monochromator, an integration sphere, and a multi-channel spectrometer. Electrospray ionization (ESI) mass spectra were recorded on a Bruker esquire 3000<sup>plus</sup> instrument. Electrochemical measurements were taken on a CH Instruments 900B potentiostat and performed using glassy carbon, platinum wire and silver wire as the working, counter, and reference electrodes, respectively. Substrates were dissolved in HPLC grade MeCN (*ca.*  $10^{-4} \text{ mol dm}^{-3}$ ) containing  $0.1 \text{ mol dm}^{-3}$  [<sup>18</sup>Bu<sub>4</sub>N][PF<sub>6</sub>] as the supporting electrolyte; all solutions were degassed with argon. Cp<sub>2</sub>Fe was used as internal reference.

Ligands **1–4**,<sup>18</sup> **11**<sup>19</sup> and **12**<sup>20</sup> were prepared as previously described. Compound **6** was synthesized by butylation of **2,2'**-

bipyridine.<sup>21</sup> [Ir(ppy)<sub>2</sub>( $\mu$ -Cl)]<sub>2</sub> was prepared by the reported method.<sup>22,23</sup>

### Device preparation

The solvents were supplied by Aldrich. The thickness of films was determined with an Ambios XP-1 profilometer. ITO-coated glass plates ( $15 \Omega \square^{-1}$ ) were patterned by conventional photolithography (<http://www.naranjosubstrates.com>) and substrates were cleaned by sonication in water-soap, water, and 2-propanol baths, in that order. After drying, the substrates were placed in a UV-ozone cleaner (Jelight 42-220) for 20 min.

To prepare the electroluminescence devices, a 90 nm layer of PEDOT:PSS (CLEVIOS<sup>TM</sup> P VP AI 4083, aqueous dispersion, 1.3–1.7% solid content, Heraeus) was first spin-coated onto the ITO glass substrate to improve device reproducibility and to prevent the formation of pinholes. Transparent films (90 nm thick) of the complexes [Ir(ppy)<sub>2</sub>(N<sup>^</sup>N)] [PF<sub>6</sub>]<sub>2</sub> with N<sup>^</sup>N = **1**, **2**, **3**, **8** and **10** and the ionic liquid 1-butyl-3-methylimidazolium hexafluorophosphate ([BMIM][PF<sub>6</sub>], >98.5%, Sigma-Aldrich) in a 4 to 1 molar ratio were spin-coated from 20 mg cm<sup>-3</sup> MeCN solution at 1000 rpm for 20 s. The devices were transferred in an inert atmosphere glovebox (<0.1 ppm O<sub>2</sub> and H<sub>2</sub>O, MBraun) and were annealed at 100 °C for 1 h. The Al electrode (70 nm) was thermally evaporated using a shadow mask under a vacuum ( $<1 \times 10^{-6} \text{ mbar}$ ) with an Edwards Auto500 evaporator integrated in the glovebox. The area of the device was 6.534 mm<sup>2</sup>. The devices were not encapsulated and were characterized inside the glovebox at room temperature.

### LEC characterization

An Avantes luminance spectrometer was used to measure the electroluminescence (EL) spectrum. Device lifetimes were measured by applying a pulsed current/DC constant voltage and monitoring voltage/current and luminance by a True Colour Sensor MAZeT (MTCsICT Sensor) with a Botest OLT OLED Lifetime-Test System (for pulsed current mode) and Keithley 2400 source meter and a photodiode coupled to a Keithley 6485 picometer using a Minolta LS100 to calibrate the photocurrent (for constant voltage mode).

**Compound 5.** Fresh KO<sup>t</sup>Bu (2.24 g, 20.0 mmol) was dissolved in dry THF (40 ml) at room temperature and 3-methylacetophenone (1.34 g, 10.0 mmol) was added. The solution turned yellow and over a period of 30 min, a precipitate formed. A solution of (*E*)-3-dimethylamino-1-(pyridin-2-yl)prop-2-en-1-one (1.76 g, 10.0 mmol) in THF (5 ml) was added and the suspension turned red immediately. The mixture was stirred for 30 min and was then left to stand overnight (*ca.* 10 h) at room temperature. Then, a solution of NH<sub>4</sub>OAc (10 g) in AcOH (20 ml) was added and the dark solution was stirred for 2 h at reflux. Solvents were reduced on a rotary evaporator and the black residue was suspended in H<sub>2</sub>O. Solid K<sub>2</sub>CO<sub>3</sub> was added until CO<sub>2</sub> evolution stopped. The aqueous phase was extracted several times into CH<sub>2</sub>Cl<sub>2</sub>, the combined organic phases were dried over MgSO<sub>4</sub> and the solvent was evaporated. The product was purified by column chromatography (SiO<sub>2</sub>, pentane–Et<sub>2</sub>O 9 : 1 changing to 2 : 3). Compound **5** was

collected as the first major fraction and was isolated as an off-white powder (1.10 g, 4.5 mmol, 45%).  $^1\text{H}$  NMR (500 MHz,  $\text{CDCl}_3$ )  $\delta$ /ppm 8.68 (ddd,  $J = 4.7, 1.9, 0.9$  Hz, 1H,  $\text{H}^{\text{E6}}$ ), 8.62 (dt,  $J = 7.8, 1.1$  Hz, 1H,  $\text{H}^{\text{E3}}$ ), 8.34 (dd,  $J = 7.8, 1.0$  Hz, 1H,  $\text{H}^{\text{F3}}$ ), 7.95 (m, 1H,  $\text{H}^{\text{G2}}$ ), 7.91 (dm,  $J = 7.8$  Hz, 1H,  $\text{H}^{\text{G6}}$ ), 7.87 (t,  $J = 7.8$  Hz, 1H,  $\text{H}^{\text{F4}}$ ), 7.83 (dt,  $J = 7.8, 1.8$  Hz, 1H,  $\text{H}^{\text{E4}}$ ), 7.75 (dd,  $J = 7.8, 1.8$  Hz, 1H,  $\text{H}^{\text{F5}}$ ), 7.38 (t,  $J = 7.6$  Hz, 1H,  $\text{H}^{\text{G5}}$ ), 7.31 (ddd,  $J = 7.4, 4.8, 1.2$  Hz, 1H,  $\text{H}^{\text{E5}}$ ), 7.24 (dm,  $J = 7.7$  Hz, 1H,  $\text{H}^{\text{G4}}$ ) 2.46 (s, 3H,  $\text{H}^{\text{Me}}$ ).  $^{13}\text{C}$  NMR (126 MHz,  $\text{CDCl}_3$ )  $\delta$ /ppm 156.6 ( $\text{C}^{\text{F6}}$ ), 156.1 ( $\text{C}^{\text{E2}}$ ), 154.7 ( $\text{C}^{\text{F2}}$ ), 149.1 ( $\text{C}^{\text{E6}}$ ), 139.3 ( $\text{C}^{\text{G1}}$ ), 138.0 ( $\text{C}^{\text{G3}}$ ), 137.6 ( $\text{C}^{\text{F4}}$ ), 137.0 ( $\text{C}^{\text{E4}}$ ), 129.8 ( $\text{C}^{\text{G4}}$ ), 128.7 ( $\text{C}^{\text{G5}}$ ), 127.7 ( $\text{C}^{\text{G2}}$ ), 124.1 ( $\text{C}^{\text{G6}}$ ), 123.8 ( $\text{C}^{\text{E5}}$ ), 121.4 ( $\text{C}^{\text{E3}}$ ), 120.5 ( $\text{C}^{\text{F5}}$ ), 119.3 ( $\text{C}^{\text{F3}}$ ), 21.6 ( $\text{C}^{\text{Me}}$ ). IR (solid,  $\nu/\text{cm}^{-1}$ ) 3051 w, 3018 w, 3012 w, 3002 w, 2955 w, 2919 w, 2857 w, 2360 m, 2321 w, 2313 w, 1700 m, 1653 m, 1607 w, 1580 s, 1560 s, 1555 m, 1506 w, 1490 w, 1472 m, 1456 m, 1447 m, 1427 s, 1420 m, 1319 w, 1287 w, 1280 w, 1258 w, 1191 w, 1156 w, 1102 w, 1084 w, 1041 w, 990 w, 826 w, 770 s, 745 w, 697 w, 668 m, 643 m, 618 m, 602 m. UV/VIS (MeCN, degassed)  $\lambda_{\text{max}}/\text{nm}$  236 ( $\epsilon/\text{dm}^3 \text{mol}^{-1} \text{cm}^{-1}$  20 700), 262 (16 500), 284 (12 700), 309sh (10 700); emission ( $\lambda_{\text{exc}} = 260$  nm)  $\lambda_{\text{em}} = 342$  nm. ESI-MS  $m/z$  246.1 [ $\text{M}$ ] $^+$  (base peak, calc. 246.1). Found C 82.11, H 5.79, N 11.76%;  $\text{C}_{17}\text{H}_{14}\text{N}_2$  requires C 81.90, H 5.73, N 11.37%.

**Compound 7.** The preparation of 7 has been reported,<sup>24</sup> but an alternative method is as follows. The procedure was as for 5 using 2-acetylpyridine (1.21 g, 5.0 mmol) and (*E*)-1-(pyrid-4-yl)-3-*N,N*-dimethylaminoprop-2-en-1-one (1.76 g, 5.0 mmol). Compound 7 was collected as the second fraction (627.0 mg, 2.7 mmol, 54%). Spectroscopic data agreed with literature data.<sup>24</sup>

**Compound 8.** The synthesis of 8 has previously been described;<sup>25</sup> we find the following method convenient. 1-(2-Oxo-2-(pyridin-2-yl)ethyl)pyridin-1-ium iodide (0.82 g, 2.5 mmol), 1,3-diphenylprop-2-en-1-one (0.52 g, 2.5 mmol) and  $\text{NH}_4\text{OAc}$  (5.78 g, 75.0 mmol) were suspended in EtOH (50 ml) and the mixture was stirred under reflux for 3 h during which time the yellow/orange colour darkened. The reaction was monitored by TLC. Solvent was evaporated to give a black residue which was suspended in  $\text{H}_2\text{O}$  and the pH was adjusted to  $\sim 8$ . The aqueous phase was extracted into  $\text{CH}_2\text{Cl}_2$  ( $3 \times 30$  ml) and the combined organic layers were washed with aqueous NaOH ( $\sim 1$  M) and water, and dried over  $\text{MgSO}_4$ . The solid was removed by filtration and the filtrate was evaporated to give a brown residue. The crude product was purified by column chromatography ( $\text{SiO}_2$ , pentane–Et $_2\text{O}$  2 : 1 changing to 1 : 4), and 8 was collected as the first fraction and isolated as a yellow solid (290 mg, 0.94 mmol, 38%). The spectroscopic data matched those reported.<sup>25</sup> UV/VIS (MeCN, degassed)  $\lambda_{\text{max}}/\text{nm}$  255 ( $\epsilon/\text{dm}^3 \text{mol}^{-1} \text{cm}^{-1}$  24 100), 316sh (4900); emission ( $\lambda_{\text{exc}} = 265$  nm)  $\lambda_{\text{em}} = 358$  nm.

**Compound 9.** 1-(2-(4-Nitrophenyl)-2-oxoethyl)pyridinium iodide (0.82 g, 2.5 mmol), (*E*)-1-(4-nitrophenyl)-3-(pyrid-2-yl)-prop-2-ene-1-one (0.52 g, 2.5 mmol) and  $\text{NH}_4\text{OAc}$  (6.24 g, 81.0 mmol) were suspended in EtOH (50 ml) and the mixture was stirred under reflux for 3 h. Solvent was removed *in vacuo* and the black residue was suspended in  $\text{H}_2\text{O}$  and the pH

adjusted to  $\sim 8$ . The aqueous phase was extracted into  $\text{CH}_2\text{Cl}_2$  ( $\sim 3 \times 30$  ml) and the combined organic layers were washed with aqueous NaOH (1 M) and  $\text{H}_2\text{O}$ , and dried over  $\text{MgSO}_4$ . The solid was separated by filtration and the filtrate was evaporated to give a brown residue. The crude product was purified using column chromatography ( $\text{SiO}_2$ , pentane–Et $_2\text{O}$  2 : 1–1 : 4, then  $\text{CH}_2\text{Cl}_2$ –MeOH 1 : 0–96 : 4). Compound 9 was obtained as the first major fraction from the chromatography column and was isolated as a yellow solid (702.0 mg, 1.76 mmol, 65%).  $^1\text{H}$  NMR (500 MHz,  $\text{DMSO-d}_6$ )  $\delta$ /ppm 8.76 (ddd,  $J = 4.7, 1.8, 0.9$  Hz, 1H,  $\text{H}^{\text{E6}}$ ), 8.75 (d,  $J = 1.6$  Hz, 1H,  $\text{H}^{\text{F3}}$ ), 8.66 (m, 2H,  $\text{H}^{\text{G2}}$ ), 8.63 (dt,  $J = 8.0, 1.1$  Hz, 1H,  $\text{H}^{\text{E3}}$ ), 8.57 (d,  $J = 1.6$  Hz, 1H,  $\text{H}^{\text{F5}}$ ), 8.38 (m, 4H,  $\text{H}^{\text{H3+G3}}$ ), 8.30 (m, 2H,  $\text{H}^{\text{H2}}$ ), 8.04 (td,  $J = 7.7, 1.8$  Hz, 1H,  $\text{H}^{\text{E4}}$ ), 7.54 (ddd,  $J = 7.4, 4.8, 1.2$  Hz, 1H,  $\text{H}^{\text{E5}}$ ).  $^{13}\text{C}$  NMR (126 MHz,  $\text{DMSO-d}_6$ )  $\delta$ /ppm 155.7 ( $\text{C}^{\text{E2/F2}}$ ), 155.6 ( $\text{C}^{\text{E2/F2}}$ ), 150.7 ( $\text{C}^{\text{E6}}$ ), 149.3 ( $\text{C}^{\text{G4+H4}}$ ), 145.4 ( $\text{C}^{\text{G1/H1}}$ ), 144.7 ( $\text{C}^{\text{G1/H1}}$ ), 139.0 ( $\text{C}^{\text{E4}}$ ), 130.2 ( $\text{C}^{\text{H2}}$ ), 129.7 ( $\text{C}^{\text{G2}}$ ), 126.0 ( $\text{C}^{\text{E5}}$ ), 125.5 ( $\text{C}^{\text{G3+H3}}$ ), 122.4 ( $\text{C}^{\text{E3}}$ ), 121.1 ( $\text{C}^{\text{F5}}$ ), 119.5 ( $\text{C}^{\text{F3}}$ ), ( $\text{C}^{\text{F4}}$  and  $\text{C}^{\text{F6}}$  not unambiguously assigned). IR (solid,  $\nu/\text{cm}^{-1}$ ) 3113 w, 3088 w, 3064 w, 2947 w, 2850 w, 2451 w, 2361 w, 1593 s, 1581 s, 1567 m, 1548 s, 1505 s, 1496 s, 1488 s, 1471 m, 1432 m, 1419 m, 1393 m, 1384 m, 1342 s, 1286 m, 1264 m, 1248 m, 1223 w, 1150 w, 1125 w, 1105 s, 1091 m, 1081 m, 1051 w, 1036 w, 1008 m, 991 m, 973 w, 958 w, 906 w, 858 s, 848 s, 836 s, 825 s, 811 s, 793 s, 753 s, 746 s, 737 s, 711 s, 691 s, 660 s, 640 s, 613 s. UV/VIS (degassed MeCN)  $\lambda_{\text{max}}/\text{nm}$  223sh ( $\epsilon/\text{dm}^3 \text{mol}^{-1} \text{cm}^{-1}$  17 600), 289 (25 200), 331sh (11 800); emission ( $\lambda_{\text{exc}} = 286$  nm)  $\lambda_{\text{em}} = 458$  nm; ESI-MS  $m/z$ : 398.1 [ $\text{M}$ ] $^+$  (base peak, calc. 398.1. Found C 65.87, H 3.65, N 14.08;  $\text{C}_{22}\text{H}_{14}\text{N}_4\text{O}_4$  requires C 66.33, H 3.54, N 14.06%.

**Compound 10.** 1-(2-Oxo-2-(pyridin-2-yl)ethyl)pyridin-1-ium iodide (0.98 g, 3.0 mmol), 1,3-di(3,4,5-trimethoxyphenyl)prop-2-en-1-one (1.17 g, 3.0 mmol) and  $\text{NH}_4\text{OAc}$  (4.00 g, 51.9 mmol) were suspended in EtOH (25 ml) and the mixture was stirred under reflux for 3 h. The yellow suspension turned black; TLC was used to monitor the reaction. The work-up was as for 9. Compound 10 was the first fraction and was isolated as a yellow solid (814 mg, 1.67 mmol, 56%).  $^1\text{H}$  NMR (500 MHz,  $\text{CDCl}_3$ )  $\delta$  (ppm) 8.73 (ddd,  $J = 4.8, 1.8, 0.9$  Hz, 1H,  $\text{H}^{\text{E6}}$ ), 8.63 (dt,  $J = 8.0, 1.1$  Hz, 1H,  $\text{H}^{\text{E3}}$ ), 8.56 (d,  $J = 1.6$  Hz, 1H,  $\text{H}^{\text{F3}}$ ), 7.88 (td,  $J = 8.0, 1.8$  Hz, 1H,  $\text{H}^{\text{E4}}$ ), 7.82 (d,  $J = 1.6$  Hz, 1H,  $\text{H}^{\text{F5}}$ ), 7.40 (s, 2H,  $\text{H}^{\text{G2}}$ ), 7.36 (ddd,  $J = 7.5, 4.8, 1.2$  Hz, 1H,  $\text{H}^{\text{E5}}$ ), 6.97 (s, 2H,  $\text{H}^{\text{H2}}$ ), 4.01 (s, 6H,  $\text{H}^{3,5\text{-OMe ring G}}$ ), 3.98 (s, 6H,  $\text{H}^{3,5\text{-OMe ring H}}$ ), 3.933 (s, 3H,  $\text{H}^{4\text{-OMe ring G}}$ ), 3.927 (s, 3H,  $\text{H}^{4\text{-OMe ring H}}$ ).  $^{13}\text{C}$  NMR (126 MHz,  $\text{CDCl}_3$ )  $\delta$ /ppm 157.1 ( $\text{C}^{\text{F6}}$ ), 156.2 ( $\text{C}^{\text{E2+F2}}$ ), 153.7 ( $\text{C}^{\text{G3/H3}}$ ), 153.6 ( $\text{C}^{\text{G3/H3}}$ ), 150.6 ( $\text{C}^{\text{F4}}$ ), 149.1 ( $\text{C}^{\text{E6}}$ ), 139.1 ( $\text{C}^{\text{G4+H4}}$ ), 136.9 ( $\text{C}^{\text{E4}}$ ), 134.7 ( $\text{C}^{\text{G1+H1}}$ ), 123.8 ( $\text{C}^{\text{E5}}$ ), 121.4 ( $\text{C}^{\text{E3}}$ ), 118.6 ( $\text{C}^{\text{F5}}$ ), 117.4 ( $\text{C}^{\text{F3}}$ ), 104.6 ( $\text{C}^{\text{G2+H2}}$ ), 60.8 ( $\text{C}^{4\text{-OMe rings G+H}}$ ), 56.4 ( $\text{C}^{3,5\text{-OMe ring G/H}}$ ), 56.3 ( $\text{C}^{3,5\text{-OMe ring G/H}}$ ). IR (solid,  $\nu/\text{cm}^{-1}$ ) 3000 m, 2939 m, 2843 w, 2825 w, 2362 m, 2333 m, 1700 m, 1653 m, 1583 s, 1545 s, 1505 s, 1456 s, 1398 m, 1383 s, 1326 s, 1245 s, 1233 s, 1201 m, 1186 m, 1167 m, 1121 s, 1092 s, 1032 m, 998 s, 962 m, 919 w, 900 w, 888 m, 851 m, 827 s, 799 s, 761 m, 729 m, 683 s, 668 s, 657 s, 625 m, 618 s. UV/VIS (degassed MeCN)  $\lambda_{\text{max}}/\text{nm}$  283 ( $\epsilon/\text{dm}^3 \text{mol}^{-1} \text{cm}^{-1}$  49 500); emission ( $\lambda_{\text{exc}} = 283$  nm)  $\lambda_{\text{em}} = 461$  nm. ESI-MS  $m/z$  488.2 [ $\text{M}$ ] $^+$

(base peak, calc. 488.2). Found C 68.13, H 5.60, N 5.79;  $C_{28}H_{28}N_2O_6$  requires C 68.84, H 5.78, N 5.73%.

### [Ir(ppy)<sub>2</sub>L][PF<sub>6</sub>]: general procedure

Unless otherwise stated, each synthesis was carried out on a 50.0  $\mu$ mol scale with respect to [Ir(ppy)<sub>2</sub>( $\mu$ -Cl)]<sub>2</sub>. In a typical reaction, [Ir(ppy)<sub>2</sub>( $\mu$ -Cl)]<sub>2</sub> (50.3 mg, 50.0  $\mu$ mol) was suspended in MeOH and ligand, L, (100.0  $\mu$ mol) was added. The solution was heated for 2 h at 120 °C in a microwave reactor. Solvent was reduced and the product precipitated by addition of solid NH<sub>4</sub>PF<sub>6</sub> (130.0 mg, 0.80 mmol). Solvent was removed and the crude product was purified by column chromatography (short column, SiO<sub>2</sub>, CH<sub>2</sub>Cl<sub>2</sub> changing to CH<sub>2</sub>Cl<sub>2</sub>-MeOH 98 : 2).

**[Ir(ppy)<sub>2</sub>(1)][PF<sub>6</sub>].** Reactants were [Ir(ppy)<sub>2</sub>( $\mu$ -Cl)]<sub>2</sub> (205.0 mg, 191.0  $\mu$ mol) and **1** (94.5 mg, 402.0  $\mu$ mol). [Ir(ppy)<sub>2</sub>(1)][PF<sub>6</sub>] was isolated as an orange powder (320.0 mg, 363.7  $\mu$ mol, 95%). <sup>1</sup>H NMR (500 MHz, 295 K, CD<sub>2</sub>Cl<sub>2</sub>)  $\delta$ /ppm 8.46 (overlapping d,  $J \approx 8.0$  Hz, 2H, H<sup>F3+E3</sup>), 8.18 (t,  $J = 7.9$  Hz, 1H, H<sup>F4</sup>), 8.10 (t,  $J = 7.9$  Hz, 1H, H<sup>E4</sup>), 7.92 (d,  $J = 8.2$  Hz, 2H, H<sup>B6+E6</sup>), 7.85 (m, 2H, H<sup>B3+B4</sup>),  $\approx 7.8$  (v br, H<sup>D3/D6</sup>, see text), 7.77 (br t,  $J = 7.4$  Hz, 1H, H<sup>D4</sup>), 7.71 (br, H<sup>D3/D6</sup>), 7.56 (d,  $J = 7.7$  Hz, 1H, H<sup>A3/C3</sup>), 7.45 (m, 2H, H<sup>A3/C3+F5</sup>), 7.38 (m, 1H, H<sup>E5</sup>), 7.08 (m, 1H, H<sup>D5</sup>), 7.03 (m, 1H, H<sup>B5</sup>), 6.96 (t,  $J = 7.5$  Hz, 1H, H<sup>A4/C4</sup>), 6.84 (t,  $J = 7.5$  Hz, 1H, H<sup>A5/C5</sup>), 6.66 (t,  $J = 7.8$  Hz, 1H, H<sup>A4/C4</sup>), 6.56 (t,  $J = 7.4$  Hz, 1H, H<sup>A5/C5</sup>), 6.01 (br d,  $J \approx 6$  Hz, 1H, H<sup>A6/C6</sup>), 5.88 (br, 1H, H<sup>G3/G4</sup>), 5.82 (d,  $J = 7.5$  Hz, 1H, H<sup>A6/C6</sup>), 5.49 (br, 1H, H<sup>G3/G4</sup>), 5.07 (v br, H<sup>G5</sup>), 3.01 (br, 3H, H<sup>NMe</sup>). <sup>13</sup>C NMR (126 MHz, 295 K, CD<sub>2</sub>Cl<sub>2</sub>)  $\delta$ /ppm 169.7 (C<sup>D2/B2</sup>), 167.8 (C<sup>D2/B2</sup>), 158.0 (C<sup>F6</sup>), 157.6 (C<sup>E2/F2</sup>), 157.55 (C<sup>E2/F2</sup>), 150.8 (C<sup>B6+E6</sup>), 150.1 (C<sup>A1/C1</sup>), 149.3 (C<sup>A1/C1</sup>), 147.4 (C<sup>A2/C2</sup>), 143.6 (C<sup>A2/C2</sup>), 139.8 (C<sup>E4</sup>), 139.6 (C<sup>F4</sup>), 138.8 (C<sup>D4</sup>), 138.5 (C<sup>B4</sup>), 131.5 (C<sup>A6/C6</sup>), 131.3 (C<sup>A3/C3</sup> or F5), 131.2 (C<sup>A5/C5</sup>), 130.9 (C<sup>A6/C6</sup>), 129.9 (C<sup>A5/C5</sup>), 128.2 (C<sup>E5</sup>), 125.5 (C<sup>E3/F3</sup>), 125.2 (C<sup>A3/C3</sup>), 124.9 (C<sup>G3/G4</sup>), 124.0 (C<sup>E3/F3</sup>), 123.8 (C<sup>D5</sup>), 123.2 (C<sup>A4/C4</sup>), 122.8 (C<sup>B5</sup>), 121.2 (C<sup>A4/C4</sup>), 120.5 (br C<sup>D3</sup>), 120.3 (C<sup>B3+(A3/C3</sup> or F5)), 112.6 (C<sup>G2</sup>), 108.7 (C<sup>G3/G4</sup>), 34.8 (C<sup>Me</sup>), signals for C<sup>G5</sup> and C<sup>D6</sup> not observed. IR (solid,  $\nu$ /cm<sup>-1</sup>) 3130 w, 3063 w, 3042 w, 2350 w, 2320 w, 1607 m, 1582 m, 1562 w, 1477 s, 1447 m, 1438 w, 1417 m, 1364 w, 1327 w, 1316 w, 1310 w, 1304 w, 1269 w, 1064 w, 1029 w, 840 s, 775 w, 757 m, 729 m, 709 m, 690 m. ESI-MS  $m/z$  735.9 [M - PF<sub>6</sub>]<sup>+</sup> (base peak calc. 736.2). Found C 50.12, H 3.46, N 7.81; C<sub>37</sub>H<sub>29</sub>F<sub>6</sub>IrN<sub>5</sub>P requires C 50.45, H 3.32, N 7.95%.

**[Ir(ppy)<sub>2</sub>(2)][PF<sub>6</sub>].** Reactants were [Ir(ppy)<sub>2</sub>( $\mu$ -Cl)]<sub>2</sub> (120.5 mg, 112.5  $\mu$ mol) and **2** (50.0 mg, 225.0  $\mu$ mol) with a reaction time of 45 min. [Ir(ppy)<sub>2</sub>(2)][PF<sub>6</sub>] was isolated as an orange powder (200.0 mg, 225.0  $\mu$ mol, 100%). <sup>1</sup>H NMR (500 MHz, 295 K, CD<sub>2</sub>Cl<sub>2</sub>)  $\delta$ /ppm 8.48 (d,  $J = 5.9$  Hz, 1H, H<sup>B6</sup>), 8.46 (d,  $J = 8.3$  Hz, 1H, H<sup>E3</sup>), 8.39 (d,  $J = 8.0$  Hz, 1H, H<sup>F3</sup>), 8.15 (t,  $J = 7.9$  Hz, 1H, H<sup>E4</sup>), 8.08 (t,  $J = 7.9$  Hz, 1H, H<sup>F4</sup>), 7.99 (d,  $J = 8.1$  Hz, 1H, H<sup>B3</sup>), 7.87 (t,  $J = 8.0$  Hz, 1H, H<sup>B4</sup>), 7.81 (m, 2H, H<sup>E6+D3</sup>), 7.73 (d,  $J = 7.8$  Hz, 1H, H<sup>D4</sup>), 7.70 (d,  $J = 7.9$  Hz, 1H, H<sup>A3/C3</sup>), 7.52 (d,  $J = 7.8$  Hz, 1H, H<sup>F5</sup>), 7.40 (m, 3H, H<sup>D6+E5+A3/C3</sup>), 7.12 (m, 1H, H<sup>B5</sup>), 7.01 (m, 2H, H<sup>A4/C4+G3/G5</sup>), 6.91 (m, 1H, H<sup>D5</sup>), 6.78 (t,  $J = 7.6$  Hz, 1H, H<sup>A5/C5</sup>), 6.69 (t,  $J = 7.8$  Hz, 1H, H<sup>A4/C4</sup>), 6.55 (t,  $J = 7.5$  Hz, 1H, H<sup>A5/C5</sup>), 6.09 (d,  $J = 3.4$  Hz, 1H, H<sup>G3/G5</sup>), 5.98 (d,  $J = 7.7$

Hz, 1H, H<sup>A6/C6</sup>), 5.90 (d,  $J = 7.6$  Hz, 1H, H<sup>A6/C6</sup>), 5.87 (d,  $J = 3.4$  Hz, 1H, H<sup>G4</sup>). <sup>13</sup>C NMR (126 MHz, 295 K, CD<sub>2</sub>Cl<sub>2</sub>)  $\delta$ /ppm 168.9 (C<sup>D2</sup>), 167.3 (C<sup>B2</sup>), 158.0 (C<sup>F2/E2</sup>), 157.6 (C<sup>F2/E2</sup>), 153.9 (C<sup>F6</sup>), 152.1 (C<sup>B6</sup>), 150.7 (C<sup>G2+E6</sup>), 149.2 (C<sup>A1/C1</sup>), 148.2 (C<sup>D6</sup>), 146.4 (C<sup>A1/C1</sup>), 144.6 (C<sup>G5/G3</sup>), 143.7 (C<sup>A2/C2</sup>), 143.3 (C<sup>A2/C2</sup>), 140.3 (C<sup>F4</sup>), 139.9 (C<sup>E4</sup>), 138.7 (C<sup>B4/D4</sup>), 138.6 (C<sup>B4/D4</sup>), 132.9 (C<sup>A6/C6</sup>), 131.4 (C<sup>A6/C6</sup>), 131.0 (C<sup>A5/C5</sup>), 130.2 (C<sup>A5/C5</sup>), 129.6 (C<sup>F5</sup>), 128.2 (C<sup>E5</sup>), 125.9 (C<sup>E3</sup>), 125.4 (C<sup>A3/C3</sup>), 124.6 (C<sup>F3</sup>), 124.2 (C<sup>A3/C3</sup>), 123.4 (C<sup>B5</sup>), 123.3 (C<sup>A4/C4</sup>), 122.9 (C<sup>D5</sup>), 121.7 (C<sup>A4/C4</sup>), 120.2 (C<sup>B3</sup>), 119.8 (C<sup>D3</sup>), 112.6 (C<sup>G3/G5</sup>), 112.1 (C<sup>G4</sup>). IR (solid,  $\nu$ /cm<sup>-1</sup>) 3124 w, 3049 w, 2335 w, 1607 m, 1582 m, 1476 m, 1437 m, 1420 m, 1317 w, 1270 w, 1226 w, 1164 m, 1125 w, 1065 m, 1031 m, 1014 m, 920 w, 885 w, 831 s, 821 s, 796 m, 754 s, 728 s. ESI-MS  $m/z$ : 723.1 [M - PF<sub>6</sub>]<sup>+</sup> (base peak calc. 723.1). Found C 49.23, H 3.10, N 6.12; C<sub>36</sub>H<sub>26</sub>F<sub>6</sub>IrN<sub>4</sub>OP·0.5H<sub>2</sub>O requires C 49.31, H 3.10, N 6.39%.

**[Ir(ppy)<sub>2</sub>(3)][PF<sub>6</sub>].** Reactants were **3** (60.0 mg, 250.0  $\mu$ mol) and [Ir(ppy)<sub>2</sub>( $\mu$ -Cl)]<sub>2</sub> (139.0 mg, 125.0  $\mu$ mol) with a reaction time of 30 min. [Ir(ppy)<sub>2</sub>(3)][PF<sub>6</sub>] was isolated as an orange powder (224.0 mg, 250.0  $\mu$ mol, 100%). <sup>1</sup>H NMR (500 MHz, 295 K, CD<sub>2</sub>Cl<sub>2</sub>)  $\delta$ /ppm 8.51 (overlapping d,  $J \approx 8.0$  Hz, 2H, H<sup>E3+F3</sup>), 8.15 (m, 2H, H<sup>E4+F4</sup>), 7.88 (m, 2H, H<sup>B3+D3</sup>), 7.85 (d,  $J = 5.5$  Hz, 1H, H<sup>E6</sup>), 7.80 (m, 3H, H<sup>B4+D4+B6/D6</sup>), 7.58 (m, 2H, H<sup>A3/C3+F5</sup>), 7.55 (d,  $J = 5.9$  Hz, 1H, H<sup>B6/D6</sup>), 7.38 (m, 2H, H<sup>A3/C3+E5</sup>), 7.10 (m, 1H, H<sup>B5/D5</sup>), 6.99 (m, 2H, H<sup>B5/D5+A4/C4</sup>), 6.90 (dd,  $J = 4.8, 1.3$  Hz, 1H, H<sup>G3/G5</sup>), 6.81 (t,  $J = 7.5$  Hz, 1H, H<sup>A5/C5</sup>), 6.67 (t,  $J = 7.5$  Hz, 1H, H<sup>A4/C4</sup>), 6.47 (t,  $J = 7.5$  Hz, 1H, H<sup>A5/C5</sup>), 6.31 (t,  $J = 4.4$  Hz, 1H, H<sup>G4</sup>), 6.22 (m, 1H, H<sup>G3/G5</sup>), 5.96 (d,  $J = 7.6$  Hz, 1H, H<sup>A6/C6</sup>), 5.72 (d,  $J = 7.6$  Hz, 1H, H<sup>A6/C6</sup>). <sup>13</sup>C NMR (126 MHz, 295 K, CD<sub>2</sub>Cl<sub>2</sub>)  $\delta$ /ppm 169.3 (C<sup>D2/B2</sup>), 167.5 (C<sup>B2/D2</sup>), 159.0 (C<sup>E2/F2</sup>), 157.6 (C<sup>E2/F2</sup>), 157.4 (C<sup>F6</sup>), 150.9 (C<sup>A1/C1</sup>), 150.8 (C<sup>B6/D6</sup>), 150.4 (C<sup>E6</sup>), 148.9 (C<sup>B6/D6</sup>), 146.6 (C<sup>A1/C1</sup>), 143.5 (C<sup>A2/C2</sup>), 143.2 (C<sup>A2/C2</sup>), 140.0 (C<sup>E4/F4</sup>), 139.9 (C<sup>E4/F4</sup>), 138.8 (C<sup>B4/D4</sup>), 138.7 (C<sup>B4/D4</sup>), 138.6 (C<sup>G2</sup>), 132.6 (C<sup>A6/C6</sup>), 131.5 (C<sup>F5</sup>), 131.2 (C<sup>A5/C5</sup>), 130.9 (C<sup>A6/C6</sup>), 130.1 (C<sup>A5/C5</sup>), 129.8 (C<sup>G3/G5</sup>), 128.3 (C<sup>E5</sup>), 128.1 (C<sup>G3/G5/G4</sup>), 128.0 (C<sup>G3/G5/G4</sup>), 125.8 (C<sup>E3/F3</sup>), 125.2 (C<sup>E3/F3</sup>), 124.7 (C<sup>A3/C3</sup>), 124.5 (C<sup>A3/C3</sup>), 123.8 (C<sup>B5/D5</sup>), 123.3 (C<sup>B5/D5</sup>), 122.9 (C<sup>A4/C4</sup>), 121.3 (C<sup>A4/C4</sup>), 120.3 (C<sup>B3/D3</sup>), 120.2 (C<sup>B3/D3</sup>). IR (solid,  $\nu$ /cm<sup>-1</sup>) 3112 w, 3049 w, 2628 w, 2326 w, 2057 w, 1982 w, 1734 w, 1717 w, 1684 m, 1653 w, 1607 s, 1583 s, 1558 s, 1477 s, 1456 s, 1439 s, 1423 s, 1419 s, 1356 w, 1318 m, 1268 m, 1263 m, 1228 m, 1164 m, 1126 w, 1063 m, 1030 m, 1010 w, 987 w, 879 w, 828 s, 798 s, 754 s, 727 s, 696 s. ESI-MS  $m/z$ : 739.1 [M - PF<sub>6</sub>]<sup>+</sup> (base peak calc. 739.1). Found C 47.87, H 3.04, N 5.89; C<sub>36</sub>H<sub>26</sub>F<sub>6</sub>IrN<sub>4</sub>PS·H<sub>2</sub>O requires C 47.94, H 3.13, N 6.21%.

**[Ir(ppy)<sub>2</sub>(4)][PF<sub>6</sub>].** Reactants were [Ir(ppy)<sub>2</sub>( $\mu$ -Cl)]<sub>2</sub> (37.4 mg, 34.9  $\mu$ mol) and **4** (20.0 mg, 69.9  $\mu$ mol); reaction time was 45 min. [Ir(ppy)<sub>2</sub>(4)][PF<sub>6</sub>] was isolated as an orange powder (62.0 mg, 66.6  $\mu$ mol, 95%). <sup>1</sup>H NMR (500 MHz, 295 K, CD<sub>2</sub>Cl<sub>2</sub>)  $\delta$ /ppm 8.50 (overlapping d,  $J \approx 8.0$  Hz, 2H, H<sup>E3+F3</sup>), 8.13 (m, 2H, H<sup>E4+F4</sup>), 7.87 (m, 3H, H<sup>B3+D3+E6</sup>), 7.81 (m, 2H, H<sup>B4+D4</sup>), 7.71 (d,  $J = 5.8$  Hz, 1H, H<sup>B6/D6</sup>), 7.64 (d,  $J = 5.5$  Hz, 1H, H<sup>G3/G5</sup>), 7.59 (m, 3H, H<sup>A3/C3+E5+B6/D6</sup>), 7.37 (m, 2H, H<sup>F5+A3/C3</sup>), 7.09 (m, 1H, H<sup>B5/D5</sup>), 6.98 (m, 2H, H<sup>B5/D5+A4/C4</sup>), 6.82 (t,  $J = 7.5$  Hz, 1H, H<sup>A5/C5</sup>), 6.68 (t,  $J = 7.5$  Hz, 1H, H<sup>A4/C4</sup>), 6.51 (m, 1H, H<sup>G4</sup>), 6.48 (t,  $J = 7.5$  Hz, 1H, H<sup>A5/C5</sup>), 6.31 (d,  $J = 3.7$  Hz, 1H, H<sup>G3/G5</sup>), 5.97

(d,  $J = 7.7$  Hz, 1H,  $H^{A6/C6}$ ), 5.74 (d,  $J = 7.7$  Hz, 1H,  $H^{A6/C6}$ ).  $^{13}\text{C}$  NMR (126 MHz, 295 K,  $\text{CD}_2\text{Cl}_2$ )  $\delta/\text{ppm}$  169.4 ( $\text{C}^{B2/D2}$ ), 167.6 ( $\text{C}^{B2/D2}$ ), 161.1 ( $\text{C}^{E2/F2/F6}$ ), 157.5 ( $\text{C}^{E2/F2/F6}$ ), 157.4 ( $\text{C}^{E2/F2/F6}$ ), 151.3 ( $\text{C}^{A1/C1}$ ), 150.8 ( $\text{C}^{B6/D6}$ ), 150.2 ( $\text{C}^{E6}$ ), 149.0 ( $\text{C}^{B6/D6}$ ), 146.7 ( $\text{C}^{A1/C1}$ ), 144.2 ( $\text{C}^{G2}$ ), 143.5 ( $\text{C}^{A2/C2}$ ), 143.2 ( $\text{C}^{A2/C2}$ ), 139.8 ( $\text{C}^{E4/F4}$ ), 138.8 ( $\text{C}^{B4/D4}$ ), 138.7 ( $\text{C}^{B4/D4}$ ), 134.3 ( $\text{C}^{G3/G5}$ ), 132.6 ( $\text{C}^{A6/C6}$ ), 132.3 ( $\text{C}^{G3/G5}$ ), 131.4 ( $\text{C}^{E5}$ ), 131.3 ( $\text{C}^{A5/C5}$ ), 130.9 ( $\text{C}^{A6/C6}$ ), 130.2 ( $\text{C}^{A5/C5+G4}$ ), 128.3 ( $\text{C}^{F5}$ ), 125.7 ( $\text{C}^{E3/F3}$ ), 125.2 ( $\text{C}^{A3/C3}$ ), 124.7 ( $\text{C}^{E3/F3}$ ), 124.4 ( $\text{C}^{A3/C3}$ ), 123.8 ( $\text{C}^{B5/D5}$ ), 123.3 ( $\text{C}^{B5/D5}$ ), 122.9 ( $\text{C}^{A4/C4}$ ), 121.4 ( $\text{C}^{A4/C4}$ ), 120.3 ( $\text{C}^{B3/D3}$ ), 120.3 ( $\text{C}^{B3/D3}$ ). IR (solid,  $\nu/\text{cm}^{-1}$ ) 3118 w, 3043 w, 2924 w, 2855 w, 2358 m, 2340 m, 2323 m, 1717 m, 1684 m, 1653 m, 1636 w, 1607 m, 1582 m, 1558 m, 1539 m, 1521 w, 1506 m, 1476 s, 1457 m, 1436 m, 1420 m, 1405 m, 1316 m, 1306 m, 1297 w, 1269 m, 1260 m, 1227 m, 1213 m, 1165 m, 1127 w, 1113 w, 1063 m, 1030 m, 1006 w, 971 w, 878 w, 831 s, 755 m, 728 s, 720 m, 692 s, 685 s, 677 s, 668 s, 652 m, 641 m. ESI-MS  $m/z$ : 785.1 [ $\text{M} - \text{PF}_6$ ] $^+$  (base peak calc. 785.1). Found C 46.40, H 2.97, N 5.82;  $\text{C}_{36}\text{H}_{26}\text{F}_6\text{IrN}_4\text{PSe}$  requires C 46.46 H 2.82 N 6.02%.

**[Ir(ppy) $_2$ (5)][PF $_6$ ].** [Ir(ppy) $_2$ (5)][PF $_6$ ] was obtained as an orange powder (89.0 mg, 100.0  $\mu\text{mol}$ , 100%).  $^1\text{H}$  NMR (500 MHz, 295 K,  $\text{CD}_2\text{Cl}_2$ )  $\delta/\text{ppm}$  8.50 (overlapping d,  $J \approx 8.0$  Hz, 2H,  $H^{E3+F3}$ ), 8.20 (t,  $J = 7.9$  Hz, 1H,  $H^{F4}$ ), 8.11 (td,  $J = 8.2$ , 1.6 Hz, 1H,  $H^{E4}$ ), 7.89 (ddd,  $J = 5.5$ , 1.6, 0.7 Hz, 1H,  $H^{E6}$ ), 7.86 (m, 2H,  $H^{B3/D3+B4/D4}$ ), 7.82 (d,  $J = 8.0$  Hz, 1H,  $H^{B3/D3}$ ), 7.76 (ddd,  $J = 8.1$ , 7.4, 1.5 Hz, 1H,  $H^{B4/D4}$ ), 7.70 (d,  $J = 5.9$  Hz, 1H,  $H^{B6/D6}$ ), 7.52 (dd,  $J = 7.7$ , 1.2 Hz, 1H,  $H^{A3/C3}$ ), 7.46 (dd,  $J = 7.7$ , 1.2 Hz, 1H,  $H^{F5}$ ), 7.38 (m, 2H,  $H^{B6/D6+E5}$ ), 7.25 (d,  $J = 7.5$  Hz, 1H,  $H^{A3/C3}$ ), 7.08 (ddd,  $J = 7.4$ , 5.9, 1.5 Hz, 1H,  $H^{B5/D5}$ ), 7.04 (m, 1H,  $H^{B5/D5}$ ), 6.95 (td,  $J = 7.7$ , 1.2 Hz, 1H,  $H^{A4/C4}$ ), 6.82 (td,  $J = 7.5$ , 1.4 Hz, 1H,  $H^{A5/C5}$ ), 6.72 (d,  $J = 7.7$  Hz, 1H,  $H^{G4}$ ), 6.64 (br t, 1H,  $H^{G5}$ ), 6.58 (td,  $J = 7.8$ , 1.2 Hz, 1H,  $H^{A4/C4}$ ), 6.42 (t,  $J = 7.3$  Hz, 1H,  $H^{A5/C5}$ ), 6.32 (v br,  $H^{G2/G6}$ , see text), 5.94 (dd,  $J = 7.8$ , 0.9 Hz, 1H,  $H^{A6/C6}$ ), 5.62 (dd,  $J = 7.8$ , 0.9 Hz, 1H,  $H^{A6/C6}$ ), 2.00 (s, 3H,  $H^{\text{Me}}$ ).  $^{13}\text{C}$  NMR (126 MHz, 295 K,  $\text{CD}_2\text{Cl}_2$ )  $\delta/\text{ppm}$  169.2 ( $\text{C}^{B2/D2}$ ), 167.6 ( $\text{C}^{B2/D2}$ ), 166.5 ( $\text{C}^{E2/F2/F6}$ ), 157.3 ( $\text{C}^{E2/F2/F6}$ ), 156.9 ( $\text{C}^{E2/F2/F6}$ ), 151.3 ( $\text{C}^{A1/C1}$ ), 150.5 ( $\text{C}^{E6}$ ), 149.2 ( $\text{C}^{B6/D6}$ ), 149.1 ( $\text{C}^{B6/D6}$ ), 147.0 ( $\text{C}^{A1/C1}$ ), 143.3 ( $\text{C}^{A2/C2}$ ), 142.9 ( $\text{C}^{A2/C2}$ ), 139.7 ( $\text{C}^{F4}$ ), 139.4 ( $\text{C}^{E4}$ ), 138.4 ( $\text{C}^{B4/D4}$ ), 138.2 ( $\text{C}^{B4/D4}$ ), 137.3 ( $\text{C}^{G3}$ ), 131.5 ( $\text{C}^{A6/C6}$ ), 131.0 ( $\text{C}^{A5/C5}$ ), 130.5 ( $\text{C}^{A6/C6}$ ), 130.3 ( $\text{C}^{G4}$ ), 130.1 ( $\text{C}^{F5}$ ), 129.4 ( $\text{C}^{A5/C5}$ ), 128.6 ( $\text{C}^{G2}$ ), 128.3 ( $\text{G}^5$ ), 127.8 ( $\text{C}^{E5}$ ), 125.2 ( $\text{C}^{E3/F3}$ ), 124.9 ( $\text{C}^{A3/C3+G6}$ ), 124.3 ( $\text{C}^{A3/C3}$ ), 123.7 ( $\text{C}^{E3/F3}$ ), 123.6 ( $\text{C}^{B5/D5}$ ), 123.0 ( $\text{C}^{A4/C4}$ ), 122.6 ( $\text{C}^{B5/D5}$ ), 121.0 ( $\text{C}^{A4/C4}$ ), 120.1 ( $\text{C}^{B3/D3}$ ), 21.3 ( $\text{C}^{\text{Me}}$ ); signal for  $\text{C}^{G1}$  not resolved. ESI-MS  $m/z$ : 747.2 [ $\text{M} - \text{PF}_6$ ] $^+$  (base peak calc. 747.2). IR (solid,  $\nu/\text{cm}^{-1}$ ) 3735 m, 3679 w, 3634 w, 3112 w, 3045 w, 2930 w, 2861 w, 2360 m, 2356 m, 2340 m, 2331 m, 2311 m, 1734 m, 1717 m, 1684 m, 1653 m, 1607 m, 1583 m, 1558 m, 1521 m, 1478 m, 1447 m, 1436 m, 1419 m, 1339 w, 1316 w, 1297 w, 1270 m, 1228 m, 1165 m, 1125 w, 1107 w, 1064 m, 1030 m, 1001 m, 879 w, 832 s, 793 m, 771 w, 755 m, 728 m, 710 m, 696 m, 677 m, 668 s, 653 m, 643 m. Found C 52.66, H 3.46, N 6.51;  $\text{C}_{39}\text{H}_{30}\text{F}_6\text{IrN}_4\text{P}$  requires C 52.52, H 3.39, N 6.28%.

**[Ir(ppy) $_2$ (6)][PF $_6$ ].** [Ir(ppy) $_2$ (6)][PF $_6$ ] was isolated as an orange powder (173.6 mg, 100.0  $\mu\text{mol}$ , 100%).  $^1\text{H}$  NMR

(500 MHz, 295 K,  $\text{CD}_2\text{Cl}_2$ )  $\delta/\text{ppm}$  8.46 (d,  $J = 8.3$  Hz, 1H,  $H^{E3}$ ), 8.38 (dd,  $J = 8.0$ , 1.0 Hz, 1H,  $H^{F3}$ ), 8.09 (m, 2H,  $H^{E4+F4}$ ), 7.99 (d,  $J = 8.0$  Hz, 1H,  $H^{B3/D3}$ ), 7.95 (d,  $J = 8.2$  Hz, 1H,  $H^{B3/D3}$ ), 7.85 (ddd,  $J = 5.5$ , 1.6, 0.7 Hz, 1H,  $H^{E6}$ ), 7.80 (m, 2H,  $H^{B4+D4}$ ), 7.71 (dd,  $J = 7.7$ , 1.3 Hz, 1H,  $H^{A3/C3}$ ), 7.67 (m, 2H,  $H^{A3/C3+B6/D6}$ ), 7.47 (dd,  $J = 7.9$ , 1.2 Hz, 1H,  $H^{F5}$ ), 7.44 (ddd,  $J = 5.9$ , 1.5, 0.8 Hz, 1H,  $H^{B6/D6}$ ), 7.35 (m, 1H,  $H^{E5}$ ), 7.04 (m, 2H,  $H^{A4/C4+B5/D5}$ ), 6.97 (m, 2H,  $H^{A4/C4+B5/D5}$ ), 6.89 (td,  $J = 7.6$ , 1.4 Hz, 1H,  $H^{A5/C5}$ ), 6.84 (td,  $J = 7.5$ , 1.3 Hz, 1H,  $H^{A5/C5}$ ), 6.23 (dd,  $J = 7.7$ , 0.8 Hz, 1H,  $H^{A6/C6}$ ), 6.05 (dd,  $J = 7.7$ , 0.8 Hz, 1H,  $H^{A6/C6}$ ), 2.62 (m, 1H,  $H^{d1/d2}$ ), 2.44 (m, 1H,  $H^{d1/d2}$ ), 1.21 (m, 1H,  $H^{c1/c2}$ ), 0.95 (m, 1H,  $H^{c1/c2}$ ), 0.73 (m, 1H,  $H^{b1/b2}$ ), 0.63 (m, 4H,  $H^{a+b1/b2}$ ).  $^{13}\text{C}$  NMR (126 MHz, 295 K,  $\text{CD}_2\text{Cl}_2$ )  $\delta/\text{ppm}$  168.2 ( $\text{C}^{B2/D2}$ ), 168.0 ( $\text{C}^{F6}$ ), 167.1 ( $\text{C}^{B2/D2}$ ), 157.3 ( $\text{C}^{E2/F2}$ ), 155.8 ( $\text{C}^{E2/F2}$ ), 151.3 ( $\text{C}^{A1/C1}$ ), 150.7 ( $\text{C}^{E6}$ ), 149.9 ( $\text{C}^{B6/D6}$ ), 148.7 ( $\text{C}^{B6/D6}$ ), 147.0 ( $\text{C}^{A1/C1}$ ), 143.1 ( $\text{C}^{A2/C2}$ ), 142.9 ( $\text{C}^{A2/C2}$ ), 140.1 ( $\text{C}^{E4/F4}$ ), 139.8 ( $\text{C}^{E4/F4}$ ), 138.6 ( $\text{C}^{B4+D4}$ ), 132.2 ( $\text{C}^{A6/C6}$ ), 131.3 ( $\text{C}^{A5/C5}$ ), 130.9 ( $\text{C}^{A5/C5}$ ), 130.6 ( $\text{C}^{A6/C6}$ ), 128.0 ( $\text{C}^{E5}$ ), 127.5 ( $\text{C}^{F5}$ ), 125.3 ( $\text{C}^{A3/C3}$ ), 125.2 ( $\text{C}^{A3/C3+E3}$ ), 123.7 ( $\text{C}^{A4/C4/B5/D5}$ ), 123.5 ( $\text{C}^{A4/C4/B5/D5}$ ), 123.0 ( $\text{C}^{A4/C4/B5/D5}$ ), 122.8 ( $\text{C}^{F3}$ ), 122.6 ( $\text{C}^{A4/C4/B5/D5}$ ), 120.3 ( $\text{C}^{B3/D3}$ ), 120.1 ( $\text{C}^{B3/D3}$ ), 40.6 ( $\text{C}^{\text{d}}$ ), 32.6 ( $\text{C}^{\text{c}}$ ), 22.2 ( $\text{C}^{\text{b}}$ ), 13.8 ( $\text{C}^{\text{a}}$ ). IR (solid,  $\nu/\text{cm}^{-1}$ ) 3118 w, 3108 w, 3043 w, 2955 w, 2927 w, 2869 w, 2858 w, 2356 s, 2340 s, 2323 s, 2311 m, 1945 w, 1923 w, 1848 w, 1829 w, 1751 m, 1734 m, 1706 m, 1695 m, 1653 m, 1636 m, 1607 s, 1582 s, 1558 s, 1550 m, 1521 m, 1506 m, 1477 s, 1456 s, 1450 s, 1439 s, 1419 s, 1405 m, 1394 m, 1374 m, 1317 m, 1303 m, 1297 w, 1269 m, 1252 w, 1228 w, 1186 w, 1165 m, 1125 w, 1099 w, 1063 m, 1030 m, 1004 w, 938 w, 878 m, 830 s, 793 s, 755 s, 736 s, 729 s, 711 m, 694 m, 668 s, 655 w, 643 m, 626 m. ESI-MS  $m/z$ : 713.2 [ $\text{M} - \text{PF}_6$ ] $^+$  (base peak calc. 713.2). Found C 49.13, H 3.84, N 6.57;  $\text{C}_{36}\text{H}_{32}\text{F}_6\text{IrN}_4\text{P}\cdot\text{H}_2\text{O}$  requires C 49.37, H 3.91, N 6.40%.

**[Ir(ppy) $_2$ (7)][PF $_6$ ].** [Ir(ppy) $_2$ (7)][PF $_6$ ] was obtained as an orange powder (87.0 mg, 100.0  $\mu\text{mol}$ , 100%).  $^1\text{H}$  NMR (500 MHz, 295 K,  $\text{CD}_2\text{Cl}_2$ )  $\delta/\text{ppm}$  8.62 (dd,  $J = 8.2$ , 1.3 Hz, 1H,  $H^{F3}$ ), 8.55 (d,  $J = 8.4$  Hz, 1H,  $H^{E3}$ ), 8.29 (t,  $J = 7.9$  Hz, 1H,  $H^{F4}$ ), 8.13 (dt,  $J = 8.0$ , 1.6 Hz, 1H,  $H^{E4}$ ), 8.01 (br d, 2H,  $H^{G2}$ ), 7.89 (m, 3H,  $H^{B3/D3+B4/D4+E6}$ ), 7.84 (d,  $J = 8.3$  Hz, 1H,  $H^{B3/D3}$ ), 7.78 (ddd,  $J = 8.2$ , 7.4, 1.5 Hz, 1H,  $H^{B4/D4}$ ), 7.68 (dt,  $J = 5.8$ , 1.2 Hz, 1H,  $H^{B6/D6}$ ), 7.55 (dd,  $J = 7.8$ , 1.3 Hz, 1H,  $H^{A3/C3}$ ), 7.45 (m, 2H,  $H^{B6/D6+F5}$ ), 7.40 (ddd,  $J = 7.6$ , 5.5, 1.2 Hz, 1H,  $H^{E5}$ ), 7.29 (dd,  $J = 7.9$ , 1.3 Hz, 1H,  $H^{A3/C3}$ ), 7.11 (m, 1H,  $H^{B5/D5}$ ), 7.06 (m, 1H,  $H^{B5/D5}$ ), 6.97 (td,  $J = 7.7$ , 1.2 Hz, 1H,  $H^{A4/C4}$ ), 6.83 (td,  $J = 7.5$ , 1.4 Hz, 1H,  $H^{A5/C5}$ ), 6.73 (dt,  $J = 7.7$ , 1.2 Hz, 1H,  $H^{C4/C4}$ ), 6.46 (td,  $J = 7.4$ , 1.3 Hz, 1H,  $H^{A5/C5} + \text{v br, } H^{G3}$ , see text), 5.94 (dd,  $J = 7.7$ , 1.1 Hz, 1H,  $H^{A6/C6}$ ), 5.62 (dd,  $J = 7.7$ , 1.1 Hz, 1H,  $H^{A6/C6}$ ).  $^{13}\text{C}$  NMR (126 MHz, 295 K,  $\text{CD}_2\text{Cl}_2$ )  $\delta/\text{ppm}$  168.8 ( $\text{C}^{B2/D2}$ ), 167.5 ( $\text{C}^{B2/D2}$ ), 163.1 ( $\text{C}^{F6}$ ), 157.6 ( $\text{C}^{E2/F2}$ ), 153.7 ( $\text{C}^{E2/F2}$ ), 151.1 ( $\text{C}^{A1/C1}$ ), 150.7 ( $\text{C}^{E6}$ ), 149.3 ( $\text{C}^{B6+D6}$ ), 149.2 ( $\text{C}^{G2}$ ), 146.4 ( $\text{C}^{A1/C1}$ ), 144.9 ( $\text{C}^{G4}$ ), 143.3 ( $\text{C}^{A2/C2}$ ), 143.1 ( $\text{C}^{A2/C2}$ ), 140.7 ( $\text{C}^{F4}$ ), 139.8 ( $\text{C}^{E4}$ ), 138.8 ( $\text{C}^{B4/D4}$ ), 138.7 ( $\text{C}^{B4/D4}$ ), 131.9 ( $\text{C}^{A6/C6}$ ), 131.2 ( $\text{C}^{A5/C5}$ ), 130.6 ( $\text{C}^{A6/C6}$ ), 130.4 ( $\text{C}^{A5/C5}$ ), 129.9 ( $\text{C}^{F5}$ ), 128.3 ( $\text{C}^{E5}$ ), 125.5 ( $\text{C}^{E3}$ ), 125.1 ( $\text{C}^{A3/C3}$ ), 125.0 ( $\text{C}^{A3/C3}$ ), 124.7 ( $\text{C}^{F3}$ ), 124.0 ( $\text{C}^{B5/D5}$ ), 123.3 ( $\text{C}^{A4/C4}$ ), 123.2 ( $\text{C}^{B5/D5}$ ), 122.6 ( $\text{C}^{G3}$ ), 121.8 ( $\text{C}^{A4/C4}$ ), 120.5 ( $\text{C}^{B3/D3}$ ), 120.4 ( $\text{C}^{B3/D3}$ ). IR (solid,  $\nu/\text{cm}^{-1}$ ) 3047 w, 2930 w, 2856 w, 2360 s, 2356 m, 2340 m, 2331 m,

2319 m, 2311 m, 1703 m, 1699 m, 1684 m, 1607 m, 1594 m, 1582 m, 1564 m, 1558 m, 1539 m, 1478 m, 1447 m, 1423 m, 1419 m, 1405 m, 1394 m, 1363 m, 1316 w, 1268 m, 1229 m, 1217 m, 1165 m, 1131 w, 1110 w, 1063 m, 1031 m, 1008 m, 877 m, 832 s, 801 m, 755 m, 736 m, 729 m, 717 m, 692 m, 668 s, 653 m, 639 m. ESI-MS  $m/z$ : 734.2  $[M - PF_6]^+$  (base peak calc. 734.2). Found C 50.03, H 3.34, N 7.88;  $C_{37}H_{27}F_6IrN_5P \cdot 0.5H_2O$  requires C 50.05, H 3.18, N 7.89%.

**[Ir(ppy)<sub>2</sub>(8)][PF<sub>6</sub>].**  $[Ir(ppy)_2(8)][PF_6]$  was isolated as an orange powder (80.0 mg, 98.9  $\mu$ mol, 98.9%). <sup>1</sup>H NMR (500 MHz, 295 K, CD<sub>2</sub>Cl<sub>2</sub>)  $\delta$ /ppm 8.69 (d,  $J = 1.9$  Hz, 1H, H<sup>F3</sup>), 8.62 (d,  $J = 8.2$  Hz, 1H, H<sup>E3</sup>), 8.14 (td,  $J = 8.1, 1.6$  Hz, 1H, H<sup>E4</sup>), 7.91 (dd,  $J = 5.5, 1.6$  Hz, 1H, H<sup>E6</sup>), 7.89 (m, 2H, H<sup>H2/H3</sup>), 7.86 (m, 2H, H<sup>B3/D3+B4/D4</sup>), 7.84 (d,  $J = 8.2$  Hz, 1H, H<sup>B3/D3</sup>), 7.76 (td,  $J = 8.2, 1.5$  Hz, 1H, H<sup>B4/D4</sup>), 7.70 (m, 2H, H<sup>B6/D6+F5</sup>), 7.61 (m, 4H, H<sup>B6/D6+H2/H3+H4</sup>), 7.54 (dd,  $J = 7.8, 1.3$  Hz, 1H, H<sup>A3/C3</sup>), 7.41 (m, 1H, H<sup>E5</sup>), 7.25 (dd,  $J = 7.8, 1.1$  Hz, 1H, H<sup>A3/C3</sup>), 7.08 (m, 1H, H<sup>B5/D5</sup>), 7.04 (m, 1H, H<sup>B5/D5</sup>), 6.97 (m, 2H, H<sup>A4/C4+G4</sup>), 6.83 (td,  $J = 7.5, 1.4$  Hz, 1H, H<sup>A5/C5</sup>), 6.76 (t,  $J = 7.7$  Hz, 2H, H<sup>G3</sup>), 6.62 (dt,  $J = 7.6, 1.2$  Hz, 1H, H<sup>A4/C4</sup>), 6.58 (br, H<sup>G2</sup>), 6.40 (td,  $J = 7.5, 1.3$  Hz, 1H, H<sup>A5/C5</sup>), 5.97 (dd,  $J = 7.8, 0.9$  Hz, 1H, H<sup>A6/C6</sup>), 5.60 (dd,  $J = 7.8, 0.9$  Hz, 1H, H<sup>A6/C6</sup>). <sup>13</sup>C NMR (126 MHz, 295 K, CD<sub>2</sub>Cl<sub>2</sub>)  $\delta$ /ppm 169.2 (C<sup>B2/D2</sup>), 167.7 (C<sup>B2/D2</sup>), 166.4 (C<sup>F2+F6</sup>), 157.3 (C<sup>E2</sup>), 151.8 (C<sup>F4</sup>), 151.7 (C<sup>A1/C1</sup>), 150.8 (C<sup>E6</sup>), 149.4 (C<sup>B6/D6</sup>), 149.3 (C<sup>B6/D6</sup>), 147.2 (C<sup>A1/C1</sup>), 143.3 (C<sup>A2/C2</sup>), 143.1 (C<sup>A2/C2</sup>), 139.7 (C<sup>E4</sup>), 138.6 (C<sup>H1</sup>), 138.55 (C<sup>B4/D4</sup>), 138.5 (C<sup>B4/D4</sup>), 138.0 (C<sup>G1</sup>), 131.8 (C<sup>A6/C6</sup>), 131.7 (C<sup>H3/H4</sup>), 131.2 (C<sup>A5/C5</sup>), 130.7 (C<sup>A6/C6</sup>), 130.2 (C<sup>H2/H3/H4</sup>), 130.1 (C<sup>A5/C5</sup>), 129.5 (C<sup>G4</sup>), 128.3 (C<sup>G3+G5</sup>), 128.0 (C<sup>G2</sup>), 127.8 (C<sup>H2/H3</sup>), 127.7 (C<sup>F5</sup>), 125.5 (C<sup>E3</sup>), 125.1 (C<sup>A3/C3</sup>), 125.0 (C<sup>A3/C3</sup>), 123.7 (C<sup>B5/D5</sup>), 123.2 (C<sup>A4/C4</sup>), 122.9 (C<sup>B5/D5</sup>), 121.3 (C<sup>F3</sup>), 121.2 (C<sup>A4/C4</sup>), 120.4 (C<sup>B3+D3</sup>). IR (solid,  $\nu/cm^{-1}$ ) 3118 w, 3108 w, 3043 w, 2955 w, 2927 w, 2869 w, 2858 w, 2356 s, 2340 s, 2323 s, 2311 w, 1981 w, 1607 m, 1582 m, 1541 m, 1533 w, 1477 s, 1451 w, 1439 m, 1423 m, 1412 m, 1397 m, 1368 w, 1364 w, 1316 w, 1307 w, 1269 w, 1243 w, 1228 w, 1164 m, 1126 w, 1064 w, 1030 m, 1021 w, 1006 w, 969 w, 877 w, 830 s, 790 m, 754 s, 745 s, 727 s, 692 s, 687 s, 675 m, 653 m. ESI-MS  $m/z$ : 809.2  $[M - PF_6]^+$  (base peak calc. 809.2). Found C 53.55, H 3.47, N 5.59;  $C_{44}H_{32}F_6IrN_4P \cdot 2H_2O$  requires C 53.38, H 3.67, N 5.66%.

**[Ir(ppy)<sub>2</sub>(9)][PF<sub>6</sub>].**  $[Ir(ppy)_2(9)][PF_6]$  was obtained as an orange powder (95.0 mg, 91.0  $\mu$ mol, 91.0%). <sup>1</sup>H NMR (500 MHz, 295 K, CD<sub>2</sub>Cl<sub>2</sub>)  $\delta$ /ppm 8.88 (d,  $J = 1.8$  Hz, 1H, H<sup>F3</sup>), 8.79 (d,  $J = 8.2$  Hz, 1H, H<sup>E3</sup>), 8.42 (d,  $J = 8.8$  Hz, 2H, H<sup>H3</sup>), 8.18 (td,  $J = 8.1, 1.5$  Hz, 1H, H<sup>E4</sup>), 8.10 (d,  $J = 8.9$  Hz, 2H, H<sup>H2</sup>), 7.90 (m, 3H, H<sup>B3/D3+B4/D4+E6</sup>), 7.86 (dd,  $J = 8.2, 0.9$  Hz, 1H, H<sup>B3/D3</sup>), 7.80 (m, 1H, H<sup>B4/D4</sup>), 7.77 (d,  $J = 5.8$  Hz, 1H, H<sup>B6/D6</sup>), 7.69 (m, 2H, H<sup>B6/D6+F5</sup>), 7.60 (br, H<sup>G3</sup>, see text), 7.56 (dd,  $J = 7.8, 1.2$  Hz, 1H, H<sup>A3/C3</sup>), 7.42 (m, 1H, H<sup>E5</sup>), 7.30–6.35 (v br, H<sup>G2+G6</sup>), 7.25 (dd,  $J = 7.8, 1.1$  Hz, 2H, H<sup>A3/C3</sup>), 7.16 (m, 1H, H<sup>B5/D5</sup>), 7.08 (m, 1H, H<sup>B5/D5</sup>), 6.97 (td,  $J = 7.7, 1.2$  Hz, 1H, H<sup>A4/C4</sup>), 6.82 (td,  $J = 7.5, 1.4$  Hz, 1H, H<sup>A5/C5</sup>), 6.63 (td,  $J = 7.8, 1.1$  Hz, 1H, H<sup>A4/C4</sup>), 6.39 (td,  $J = 7.4, 1.3$  Hz, 1H, H<sup>A5/C5</sup>), 5.92 (dd,  $J = 7.7, 0.9$  Hz, 1H, H<sup>A6/C6</sup>), 5.59 (dd,  $J = 7.7, 0.8$  Hz, 1H, H<sup>A6/C6</sup>). <sup>13</sup>C NMR (126 MHz, 295 K, CD<sub>2</sub>Cl<sub>2</sub>)  $\delta$ /ppm 168.4 (C<sup>B2/D2</sup>), 167.0 (C<sup>B2/D2</sup>), 163.6 (C<sup>F6</sup>), 158.2 (C<sup>E2/F2</sup>), 156.2 (C<sup>E2/F2</sup>), 150.7 (C<sup>A1/C1</sup>), 150.6

(C<sup>E6</sup>), 150.0 (C<sup>H4</sup>), 149.4 (C<sup>H1</sup>), 149.3 (C<sup>B6/D6</sup>), 149.2 (C<sup>B6/D6</sup>), 146.1 (C<sup>A1/C1</sup>), 143.0 (C<sup>A2/C2</sup>), 142.9 (C<sup>A2/C2</sup>), 139.7 (C<sup>E4</sup>), 138.7 (C<sup>B4/D4</sup>), 138.5 (C<sup>B4/D4</sup>), 132.2 (C<sup>A6/C6</sup>), 131.0 (C<sup>A5/C5</sup>), 130.3 (C<sup>A6/C6</sup>), 129.9 (C<sup>A5/C5</sup>), 129.1 (C<sup>H2</sup>), 128.4 (C<sup>E5</sup>), 127.2 (C<sup>F5</sup>), 126.1 (C<sup>E3</sup>), 124.9 (C<sup>H3</sup>), 124.8 (C<sup>A3/C3</sup>), 124.4 (C<sup>A3/C3</sup>), 123.9 (C<sup>B5/D5</sup>), 123.4 (C<sup>G3+G5</sup>, see text), 123.2 (C<sup>A4/C4</sup>), 123.1 (C<sup>B5/D5</sup>), 122.6 (C<sup>F3</sup>), 120.8 (C<sup>A4/C4</sup>), 120.2 (C<sup>B3+D3</sup>), signal for C<sup>F4</sup> not resolved; signals for C<sup>G2/G6</sup>, C<sup>G1</sup> or C<sup>G4</sup> not observed at 295 K; at 210 K: 128.8 (C<sup>G2/G6</sup>), 128.3 (C<sup>G2/G6</sup>), 122.9 (C<sup>G3+G5</sup>). IR (solid,  $\nu/cm^{-1}$ ) 3120 w, 3108 w, 3055 w, 2965 w, 2937 w, 2879 w, 2860 w, 2356 s, 2340 s, 2323 s, 2311 m, 1945 w, 1923 w, 1848 w, 1829 w, 1751 m, 1734 m, 1700 m, 1607 m, 1583 m, 1544 w, 1512 m, 1506 m, 1477 m, 1453 w, 1438 w, 1422 m, 1419 m, 1395 w, 1344 m, 1317 m, 1309 w, 1295 w, 1269 w, 1228 w, 1164 w, 1126 w, 1108 w, 1064 w, 1030 m, 1014 w, 1006 w, 994 w, 828 s, 820 s, 801 m, 789 m, 752 s, 728 s, 721 m, 694 s, 687 m, 675 m, 668 m, 652 m, 641 w. ESI-MS  $m/z$ : 899.3  $[M - PF_6]^+$  (base peak calc. 899.2). Found C 50.41, H 2.96, N 8.00;  $C_{44}H_{30}F_6IrN_6O_4P$  requires C 50.62, H 2.90, N 8.05%.

**[Ir(ppy)<sub>2</sub>(10)][PF<sub>6</sub>].**  $[Ir(ppy)_2(10)][PF_6]$  was obtained as an orange powder (112.0 mg, 98.8  $\mu$ mol, 98.8%). <sup>1</sup>H NMR (500 MHz, 295 K, CD<sub>2</sub>Cl<sub>2</sub>)  $\delta$ /ppm 8.69 (d,  $J = 8.3$  Hz, 1H, H<sup>E3</sup>), 8.65 (d,  $J = 2.0$  Hz, 1H, H<sup>F3</sup>), 8.15 (td,  $J = 8.2, 1.6$  Hz, 1H, H<sup>E4</sup>), 7.97 (m, 3H, H<sup>E6+B3+D3</sup>), 7.85–7.76 (m, 3H, H<sup>B4+D4+B6/D6</sup>), 7.72 (ddd,  $J = 5.8, 1.6, 0.8$  Hz, 1H, H<sup>B6/D6</sup>), 7.60 (d,  $J = 2.0$  Hz, 1H, H<sup>F5</sup>), 7.57 (d,  $J = 6.6$  Hz, 1H, H<sup>A3/C3</sup>), 7.38 (ddd,  $J = 7.6, 5.5, 1.1$  Hz, 1H, H<sup>E5</sup>), 7.33 (dd,  $J = 7.3, 1.1$  Hz, 1H, H<sup>A3/C3</sup>), 7.12 (m, 1H, H<sup>B5/D5</sup>), 7.06 (m overlapping s, 3H, H<sup>B5/D5+H2</sup>), 6.97 (td,  $J = 7.4, 1.6$  Hz, 1H, H<sup>A4/C4</sup>), 6.82 (td,  $J = 7.6, 1.4$  Hz, 1H, H<sup>A5/C5</sup>), 6.65 (td,  $J = 7.8, 1.2$  Hz, 1H, H<sup>A4/C4</sup>), 6.50 (td,  $J = 7.5, 1.3$  Hz, 1H, H<sup>A5/C5</sup>), 6.34 (br, 1H, H<sup>G2/G6</sup>), 5.92 (ddd,  $J = 7.7, 1.2, 0.5$  Hz, 1H, H<sup>A6/C6</sup>), 5.74 (ddd,  $J = 7.6, 1.2, 0.5$  Hz, 1H, H<sup>A6/C6</sup>), 5.38 (br, 1H, H<sup>G2/G6</sup>), 3.95 (s, 6H, H<sup>OMe3 ring H</sup>), 3.86 (s, 3H, H<sup>OMe4 ring G/H</sup>), 3.69 (s, 3H, H<sup>OMe4 ring G/H</sup>), 3.63 (br, 3H, H<sup>OMe3/5 ring G</sup>), 3.36 (br, 3H, H<sup>OMe3/5 ring G</sup>). <sup>13</sup>C NMR (126 MHz, 295 K, CD<sub>2</sub>Cl<sub>2</sub>)  $\delta$ /ppm 168.7 (C<sup>B2/D2</sup>), 167.3 (C<sup>B2/D2</sup>), 165.4 (C<sup>F6</sup>), 156.8 (C<sup>E2+F2</sup>), 154.2 (C<sup>H3</sup>), 152.2 (C<sup>G3/G5</sup>), 152.0 (C<sup>F4</sup>), 151.6 (C<sup>G3/G5</sup>), 150.8 (C<sup>A1/C1</sup>), 150.7 (C<sup>E6</sup>), 149.7 (C<sup>B6/D6</sup>), 149.4 (C<sup>B6/D6</sup>), 147.3 (C<sup>A1/C1</sup>), 143.0 (C<sup>A2/C2</sup>), 142.4 (C<sup>A2/C2</sup>), 140.7 (C<sup>G4/H4</sup>), 139.7 (C<sup>E4</sup>), 138.7 (C<sup>B4/D4</sup>), 138.5 (C<sup>B4/D4</sup>), 137.4 (C<sup>G4/H4</sup>), 131.3 (C<sup>A5/C5</sup>), 131.6 (C<sup>A6/C6</sup>), 130.7 (C<sup>A6/C6</sup>), 130.6 (C<sup>H1</sup>), 129.5 (C<sup>A5/C5</sup>), 128.9 (C<sup>G1</sup>), 128.2 (C<sup>E5</sup>), 127.4 (C<sup>F5</sup>), 125.9 (C<sup>E3</sup>), 125.2 (C<sup>A3/C3</sup>), 123.9 (C<sup>A3/C3</sup>), 123.7 (C<sup>B5/D5</sup>), 123.1 (C<sup>A4/C4</sup>), 122.9 (C<sup>B5/D5</sup>), 121.4 (C<sup>A4/C4</sup>), 121.3 (C<sup>F3</sup>), 120.1 (C<sup>B3+D3</sup>), 106.2 (C<sup>G2/G6</sup>), 105.9 (C<sup>G2/G6</sup>), 105.1 (C<sup>H2</sup>), 61.1 (C<sup>OMe4 ring G/H</sup>), 60.2 (C<sup>OMe4 ring G/H</sup>), 56.9 (C<sup>OMe3 ring H</sup>), 56.0 (C<sup>OMe3/5 ring G</sup>), 55.9 (C<sup>OMe3/5 ring G</sup>). IR (solid,  $\nu/cm^{-1}$ ) 3055 w, 2997 w, 2935 w, 2840 w, 1702 w, 1606 m, 1583 m, 1568 w, 1564 w, 1538 w, 1504 m, 1477 m, 1453 m, 1440 w, 1393 m, 1330 m, 1318 w, 1306 w, 1268 w, 1238 m, 1164 w, 1122 m, 1108 m, 1101 m, 1059 w, 1030 w, 998 m, 968 w, 827 s, 804 m, 787 m, 756 m, 749 m, 728 m, 676 m, 669 m, 659 m, 653 m, 639 w. ESI-MS  $m/z$ : 989.4  $[M - PF_6]^+$  (base peak calc. 989.3). Found C 52.36, H 3.92, N 4.83;  $C_{50}H_{44}F_6IrN_4O_6P$  requires C 52.92, H 3.91, N 4.94%.

**[Ir(ppy)<sub>2</sub>(11)][PF<sub>6</sub>].** The reactants were  $[Ir(ppy)_2(\mu-Cl)]_2$  (102.5 mg, 95.7  $\mu$ mol) and **11** (50.0 mg, 191.1  $\mu$ mol) with a

reaction time of 1 h.  $[\text{Ir}(\text{ppy})_2(\mathbf{11})][\text{PF}_6]$  was isolated as a red solid (56.0 mg, 61.2  $\mu\text{mol}$ , 32.0%).  $^1\text{H}$  NMR (500 MHz, 295 K,  $\text{CD}_2\text{Cl}_2$ )  $\delta/\text{ppm}$  9.07 (d,  $J = 1.8$  Hz, 1H,  $\text{H}^{\text{F6}}$ ), 8.84 (dd,  $J = 8.4$ , 2.0 Hz, 1H,  $\text{H}^{\text{F4}}$ ), 8.62 (m, 2H,  $\text{H}^{\text{E3+F3}}$ ), 8.44 (d,  $J = 4.7$  Hz, 1H,  $\text{H}^{\text{G6}}$ ), 8.19 (td,  $J = 8.0$ , 1.6 Hz, 1H,  $\text{H}^{\text{E4}}$ ), 8.08 (m, 2H,  $\text{H}^{\text{E6+G3}}$ ), 7.98 (m, 2H,  $\text{H}^{\text{B3+D3}}$ ), 7.91 (td,  $J = 7.7$ , 1.7 Hz, 1H,  $\text{H}^{\text{G4}}$ ), 7.80 (t,  $J = 7.8$  Hz, 2H,  $\text{H}^{\text{B4+D4}}$ ), 7.76 (d,  $J = 7.9$  Hz, 1H,  $\text{H}^{\text{A3/C3}}$ ), 7.73 (d,  $J = 7.8$  Hz, 1H,  $\text{H}^{\text{A3/C3}}$ ), 7.60 (d,  $J = 5.6$  Hz, 1H,  $\text{H}^{\text{B6/D6}}$ ), 7.52 (m, 3H,  $\text{H}^{\text{B6/D6+E5+G5}}$ ), 7.09 (td,  $J = 7.7$ , 1.2 Hz, 1H,  $\text{H}^{\text{A4/C4}}$ ), 7.03 (m, 3H,  $\text{H}^{\text{A4/C4+B5+D5}}$ ), 6.96 (td,  $J = 7.4$ , 1.3 Hz, 1H,  $\text{H}^{\text{A5/C5}}$ ), 6.91 (td,  $J = 7.5$ , 1.3 Hz, 1H,  $\text{H}^{\text{A5/C5}}$ ), 6.33 (overlapping d,  $J = 7.6$  Hz, 2H,  $\text{H}^{\text{A6+C6}}$ ).  $^{13}\text{C}$  NMR (126 MHz, 295 K,  $\text{CD}_2\text{Cl}_2$ )  $\delta/\text{ppm}$  188.3 ( $\text{C}^{\text{C=O}}$ ), 168.3 ( $\text{C}^{\text{B2/D2}}$ ), 167.2 ( $\text{C}^{\text{B2/D2}}$ ), 158.2 ( $\text{C}^{\text{E2/F2}}$ ), 155.4 ( $\text{C}^{\text{E2/F2}}$ ), 154.6 ( $\text{C}^{\text{F6}}$ ), 153.1 ( $\text{C}^{\text{G2}}$ ), 151.6 ( $\text{C}^{\text{E6}}$ ), 150.1 ( $\text{C}^{\text{A1/C1}}$ ), 150.0 ( $\text{C}^{\text{A1/C1}}$ ), 149.2 ( $\text{C}^{\text{B6+D6}}$ ), 149.1 ( $\text{C}^{\text{G6}}$ ), 144.25 ( $\text{C}^{\text{A2/C2}}$ ), 144.2 ( $\text{C}^{\text{A2/C2}}$ ), 141.7 ( $\text{C}^{\text{F4}}$ ), 140.1 ( $\text{C}^{\text{E4}}$ ), 138.9 ( $\text{C}^{\text{B4/D4}}$ ), 138.8 ( $\text{C}^{\text{B4/D4}}$ ), 138.1 ( $\text{C}^{\text{G4}}$ ), 136.0 ( $\text{C}^{\text{F5}}$ ), 132.2 ( $\text{C}^{\text{A6/C6}}$ ), 132.1 ( $\text{C}^{\text{A6/C6}}$ ), 131.3 ( $\text{C}^{\text{A5/C5}}$ ), 131.2 ( $\text{C}^{\text{A5/C5}}$ ), 129.6 ( $\text{C}^{\text{E5/G5}}$ ), 128.1 ( $\text{C}^{\text{E5/G5}}$ ), 126.2 ( $\text{C}^{\text{E3/F3}}$ ), 125.5 ( $\text{C}^{\text{A3/C3}}$ ), 125.4 ( $\text{C}^{\text{A3/C3}}$ ), 125.1 ( $\text{C}^{\text{G3}}$ ), 124.4 ( $\text{C}^{\text{E3/F3}}$ ), 124.0 ( $\text{C}^{\text{B5/D5}}$ ), 123.9 ( $\text{C}^{\text{B5/D5}}$ ), 123.4 ( $\text{C}^{\text{A4/C4}}$ ), 123.35 ( $\text{C}^{\text{A4/C4}}$ ), 120.5 ( $\text{C}^{\text{B3/D3}}$ ), 120.4 ( $\text{C}^{\text{B3/D3}}$ ). IR (solid,  $\nu/\text{cm}^{-1}$ ) 3059 w, 2920 m, 2850 m, 2361 w, 1717 m, 1674 m, 1668 m, 1662 m, 1607 s, 1582 s, 1563 m, 1558 m, 1553 m, 1478 s, 1468 m, 1464 m, 1436 m, 1419 m, 1379 m, 1360 m, 1308 m, 1284 m, 1270 m, 1246 m, 1228 m, 1165 m, 1141 w, 1127 w, 1114 w, 1092 w, 1065 m, 1032 m, 996 m, 947 m, 878 m, 830 s, 801 s, 795 s, 750 s, 738 s, 730 s, 719 s, 698 s, 678 s, 662 m, 619 m. ESI-MS  $m/z$ : 762.2  $[\text{M} - \text{PF}_6]^+$  (base peak calc. 762.2). Found C 49.61 H 3.10 N 7.74;  $\text{C}_{38}\text{H}_{27}\text{F}_6\text{IrN}_5\text{OP}\cdot\text{MeOH}$  requires C 49.89 H 3.33 N 7.46%.

$[\text{Ir}(\text{ppy})_2(\mathbf{12})][\text{PF}_6]$ . Reactants were  $\mathbf{12}$  (16.4 mg, 93.0  $\mu\text{mol}$ ) and  $[\text{Ir}(\text{ppy})_2(\mu\text{-Cl})_2]$  (50.0 mg, 47.0  $\mu\text{mol}$ ) with a reaction time of 1 h.  $[\text{Ir}(\text{ppy})_2(\mathbf{12})][\text{PF}_6]$  was isolated as a dark red powder (61.8 mg, 74.4  $\mu\text{mol}$ , 80.0%).  $^1\text{H}$  NMR (500 MHz, 295 K,  $\text{CD}_2\text{Cl}_2$ )  $\delta/\text{ppm}$  8.41 (d,  $J = 8.0$  Hz, 1H,  $\text{H}^{\text{E3}}$ ), 8.26 (m, 2H,  $\text{H}^{\text{B6/D6+c}}$ ), 8.07 (t,  $J = 7.7$  Hz, 1H,  $\text{H}^{\text{E4}}$ ), 7.97 (m, 2H,  $\text{H}^{\text{B3/D3+E6}}$ ), 7.92 (d,  $J = 8.1$  Hz, 1H,  $\text{H}^{\text{B3/D3}}$ ), 7.80 (m, 2H,  $\text{H}^{\text{B4+D4}}$ ), 7.68 (m, 2H,  $\text{H}^{\text{A3+C3}}$ ), 7.47 (m, 1H,  $\text{H}^{\text{E5}}$ ), 7.44 (d,  $J = 5.9$  Hz, 1H,  $\text{H}^{\text{B6/D6}}$ ), 7.18 (dd,  $J = 7.4$ , 5.8 Hz, 1H,  $\text{H}^{\text{B5/D5}}$ ), 7.04 (m, 1H,  $\text{H}^{\text{B5/D5}}$ ), 6.99 (m, 2H,  $\text{H}^{\text{A4+C4}}$ ), 6.84 (m, 2H,  $\text{H}^{\text{A5+C5}}$ ), 6.27 (d,  $J = 7.6$  Hz, 1H,  $\text{H}^{\text{A6/C6}}$ ), 6.20 (m, 2H,  $\text{H}^{\text{A6/C6+d}}$ ), 3.38 (s, 3H,  $\text{H}^{\text{Me}}$ ), 3.26 (s, 3H,  $\text{H}^{\text{Me}}$ ).  $^{13}\text{C}$  NMR (126 MHz, 295 K,  $\text{CD}_2\text{Cl}_2$ )  $\delta/\text{ppm}$  186.9 ( $\text{C}^{\text{C=O}}$ ), 169.0 ( $\text{C}^{\text{B2/D2}}$ ), 167.9 ( $\text{C}^{\text{B2/D2}}$ ), 159.8 ( $\text{C}^{\text{C}}$ ), 155.2 ( $\text{C}^{\text{E2}}$ ), 150.6 ( $\text{C}^{\text{E6}}$ ), 148.9 ( $\text{C}^{\text{B6/D6}}$ ), 148.85 ( $\text{C}^{\text{B6/D6}}$ ), 145.2 ( $\text{C}^{\text{A1+C1}}$ ), 144.9 ( $\text{C}^{\text{A2/C2}}$ ), 144.2 ( $\text{C}^{\text{A2/C2}}$ ), 139.2 ( $\text{C}^{\text{E4}}$ ), 138.6 ( $\text{C}^{\text{B4/D4}}$ ), 138.4 ( $\text{C}^{\text{B4/D4}}$ ), 133.0 ( $\text{C}^{\text{A6/C6}}$ ), 132.1 ( $\text{C}^{\text{A6/C6}}$ ), 130.4 ( $\text{C}^{\text{A5+C5}}$ ), 130.0 ( $\text{C}^{\text{E5}}$ ), 127.5 ( $\text{C}^{\text{E3}}$ ), 125.3 ( $\text{C}^{\text{A3/C3}}$ ), 124.9 ( $\text{C}^{\text{A3/C3}}$ ), 123.5 ( $\text{C}^{\text{B5/D5}}$ ), 123.4 ( $\text{C}^{\text{B5/D5}}$ ), 122.8 ( $\text{C}^{\text{A4/C4}}$ ), 122.4 ( $\text{C}^{\text{A4/C4}}$ ), 120.0 ( $\text{C}^{\text{B3/D3}}$ ), 119.9 ( $\text{C}^{\text{B3/D3}}$ ), 93.6 ( $\text{C}^{\text{d}}$ ), 47.2 ( $\text{C}^{\text{Me}}$ ), 39.3 ( $\text{C}^{\text{Me}}$ ). IR (solid,  $\nu/\text{cm}^{-1}$ ) 3125 w, 3056 w, 2931 w, 2862 w, 2358 w, 2329 w, 1630 s, 1607 s, 1600 m, 1582 m, 1565 m, 1517 s, 1496 s, 1490 s, 1475 s, 1465 m, 1456 m, 1439 m, 1405 s, 1375 m, 1363 m, 1299 m, 1259 s, 1252 s, 1245 s, 1227 m, 1161 m, 1141 m, 1127 m, 1119 m, 1102 m, 1083 m, 1062 m, 1054 m, 1044 m, 1031 m, 1023 m, 1012 m, 984 m, 967 m, 958 w, 938 w, 906 m, 887 m, 882 m, 865 m, 832 s, 792 m, 771 m, 756 s, 735 s, 729 s,

722 s, 712 m, 694 s, 682 s, 668 s, 655 m, 630 m. ESI-MS  $m/z$ : 677.2  $[\text{M} - \text{PF}_6]^+$  (base peak, calc. 677.2). Found C 46.96, H 3.82, N 6.53;  $\text{C}_{32}\text{H}_{28}\text{F}_6\text{IrN}_4\text{OP}$  requires C 46.77, H 3.43, N 6.82%.

### Crystallography

Data were collected on a Stoe IPDS diffractometer using Stoe IPDS<sup>26</sup> software and the program SHELXL97,<sup>27</sup> or on a Bruker-Nonius KappaAPEX diffractometer with data reduction, solution and refinement using the programs APEX2,<sup>28</sup> SIR92,<sup>29</sup> and CRYSTALS.<sup>30</sup> ORTEP-type diagrams and structure analysis used Mercury v. 3.0.<sup>31,32</sup> Data are given in Table 1. In  $2\{[\text{Ir}(\text{ppy})_2(\mathbf{9})][\text{PF}_6]\cdot\text{CH}_2\text{Cl}_2\cdot 2\text{H}_2\text{O}$  and  $2\{[\text{Ir}(\text{ppy})_2(\mathbf{12})][\text{PF}_6]\cdot\text{MeOH}\cdot 2\text{H}_2\text{O}$ , partial occupancy water solvates were modelled as naked O atoms as data quality did not allow location of the H atoms from the difference map.

## Results and discussion

### Ligand synthesis and characterization

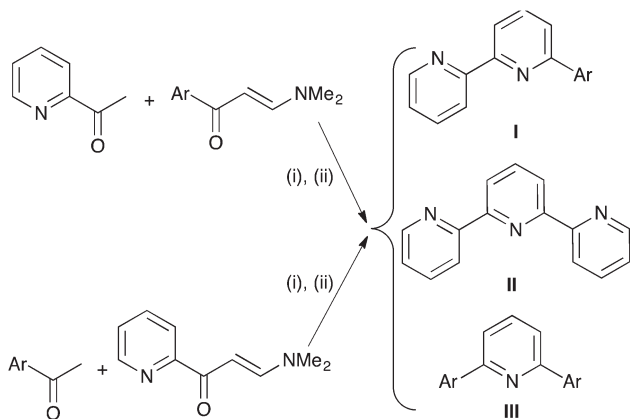
Of the twelve ligands used in this investigation, compounds **5**, **9** and **10** have not been previously reported. Ligands **8**, **9** and **10** were prepared by standard Kröhnke methodology.<sup>33</sup> We approached the synthesis of **5** using the strategy described by Jahng *et al.*<sup>34,35</sup> This involves a multistep and multicomponent reaction consisting of the *in situ* preparation of an enolate which reacts then in a Michael condensation with an enamionone followed by elimination of dimethylamine to give a 1,5-bis(aryl)pentane-1,5-diketone. This reacts further upon addition of  $\text{NH}_4\text{OAc}$  in cascade imine condensations leading to ring closure to a dihydropyridine; subsequent oxidation yields a 2,6-bis(aryl)pyridine. Two approaches can be used, and these are summarized in Scheme 2. A disadvantage of the methodology is the reversibility of the Michael addition resulting in scrambling of the substituents and competitive formation of 6'-aryl-2,2'-bpy (**I**), 2,2':6',2''-terpyridine (tpy, **II**) and 2,6-bis(aryl)-pyridine (**III**). In the synthesis of **5**, the lower route in Scheme 2 was the most effective with **5** and tpy (**I** and **II** in Scheme 2) being isolated in 54 and 20% yields, respectively, and no 2,6-bis(3-tolyl)-pyridine (**III** in Scheme 2) being formed. The Jahng methodology was also found to be a convenient route for compound **7** for which the more efficient strategy was the upper one in Scheme 2, starting from 2-acetylpyridine and (*E*)-1-(pyrid-4-yl)-3-*N,N*-dimethylaminoprop-2-ene-1-one; compound **7** was isolated in 45% yield with only 4% of 4,2':6',4''-terpyridine (product **III** in Scheme 2) as byproduct.

The EI mass spectra of **5**, **9** and **10** each exhibited a parent ion. The  $^1\text{H}$  and  $^{13}\text{C}$  NMR spectra of the new ligands were assigned using COSY, NOESY, DEPT, HMQC and HMBC methods and were fully in accord with the structures drawn in Scheme 1 and with unhindered bond rotation on the NMR timescale. For example in **10**, four signals at  $\delta$  4.01, 3.98, 3.933 and 3.927 ppm (integral ratio 2:2:1:1) were observed at 295 K for the six methoxy groups.

**Table 1** Crystallographic data for ligands **9** and **10** (two polymorphs) and the complexes

Compound	<b>9</b>	<b>10a</b>	<b>10b</b>
Formula	C <sub>22</sub> H <sub>14</sub> N <sub>4</sub> O <sub>4</sub>	C <sub>28</sub> H <sub>28</sub> N <sub>2</sub> O <sub>6</sub>	C <sub>28</sub> H <sub>28</sub> N <sub>2</sub> O <sub>6</sub>
Formula weight	398.37	488.54	488.54
Crystal colour and habit	Yellow block	Colourless prism	Colourless needle
Crystal system	Monoclinic	Triclinic	Monoclinic
Space group	<i>P2<sub>1</sub>/c</i>	<i>P1</i>	<i>P2<sub>1</sub>/c</i>
<i>a</i> , <i>b</i> , <i>c</i> /Å	20.196(8), 7.0193(16), 13.309(6)	10.5992(2), 11.0302(2), 12.2247(3)	13.0887(7), 17.9889(8), 10.9843(8)
$\alpha$ , $\beta$ , $\gamma$ /°	90, 106.79(3), 90	96.3390(10), 108.9380(10), 108.6850(10)	90, 108.615(3), 90
<i>U</i> /Å <sup>3</sup>	1806.3(11)	1243.40(5)	2451.0(3)
<i>D<sub>c</sub></i> /Mg m <sup>-3</sup>	1.465	1.305	1.324
<i>Z</i>	4	2	4
$\mu$ (Mo-K $\alpha$ )/mm <sup>-1</sup>	0.104	0.092	0.094
<i>T</i> /K	173	123	123
Refln. collected	17 964	43 182	27 283
Unique refln. ( <i>R</i> <sub>int</sub> )	3189 (0.1149)	11 963 (0.023)	5624 (0.054)
Refln. for refinement	2573	9173	3375
Parameters	273	325	325
Threshold	<i>I</i> > 2 $\sigma$ ( <i>I</i> )	<i>I</i> > 2 $\sigma$ ( <i>I</i> )	<i>I</i> > 2 $\sigma$ ( <i>I</i> )
<i>R</i> <sub>1</sub> ( <i>R</i> <sub>1</sub> all data)	0.1076 (0.1260)	0.0446 (0.0539)	0.0397 (0.0842)
<i>wR</i> <sub>2</sub> ( <i>wR</i> <sub>2</sub> all data)	0.3112 (0.3266)	0.0496 (0.0766)	0.0398 (0.0879)
Goodness of fit	1.070	1.0538	1.1104
CCDC deposition	910293	910297	910295

Compound	2{[Ir(ppy) <sub>2</sub> ( <b>1</b> )]- [PF <sub>6</sub> ]}·C <sub>6</sub> H <sub>5</sub> Me	2{[Ir(ppy) <sub>2</sub> ( <b>9</b> )]- [PF <sub>6</sub> ]}·CH <sub>2</sub> Cl <sub>2</sub> ·2H <sub>2</sub> O	[Ir(ppy) <sub>2</sub> ( <b>10</b> )] [PF <sub>6</sub> ]	2{[Ir(ppy) <sub>2</sub> ( <b>12</b> )]- [PF <sub>6</sub> ]}·MeOH·2H <sub>2</sub> O
Formula	C <sub>81</sub> H <sub>66</sub> F <sub>12</sub> Ir <sub>2</sub> N <sub>10</sub> P <sub>2</sub>	C <sub>89</sub> H <sub>66</sub> Cl <sub>2</sub> F <sub>12</sub> Ir <sub>2</sub> N <sub>12</sub> O <sub>10</sub> P <sub>2</sub>	C <sub>50</sub> H <sub>44</sub> F <sub>6</sub> IrN <sub>4</sub> O <sub>6</sub> P	C <sub>65</sub> H <sub>64</sub> F <sub>12</sub> Ir <sub>2</sub> N <sub>8</sub> O <sub>5</sub> P <sub>2</sub>
Formula weight	1853.78	2208.83	1134.08	1711.59
Crystal colour and habit	Orange block	Orange plate	Orange block	Red block
Crystal system	Orthorhombic	Triclinic	Monoclinic	Monoclinic
Space group	<i>Pbcn</i>	<i>P1</i>	<i>P2<sub>1</sub>/n</i>	<i>P2<sub>1</sub>/c</i>
<i>a</i> , <i>b</i> , <i>c</i> /Å	20.941(4), 20.129(4), 16.916(3)	9.776(3), 14.684(5), 17.409(5)	12.5203(8), 18.8096(10), 18.9682(13)	16.4951(12), 13.0662(11), 16.4258(11)
$\alpha$ , $\beta$ , $\gamma$ /°	90, 90, 90	74.15(2), 76.01(2), 72.54(2)	90, 95.328(5), 90	90, 113.986(5), 90
<i>U</i> /Å <sup>3</sup>	7130(2)	2258.2(12)	4447.7(5)	3234.5(4)
<i>D<sub>c</sub></i> /Mg m <sup>-3</sup>	1.727	1.645	1.694	1.753
<i>Z</i>	4	1	4	2
$\mu$ (Mo-K $\alpha$ )/mm <sup>-1</sup>	3.860	3.130	3.120	4.251
<i>T</i> /K	173	173	173	173
Refln. collected	123 452	30 520	77 004	22 644
Unique refln. ( <i>R</i> <sub>int</sub> )	7385 (0.0734)	9370 (0.1209)	10 213 (0.0874)	7004 (0.0589)
Refln. for refinement	6759	8294	9844	6568
Parameters	529	622	619	446
Threshold	<i>I</i> > 2 $\sigma$ ( <i>I</i> )	<i>I</i> > 2 $\sigma$ ( <i>I</i> )	<i>I</i> > 2 $\sigma$ ( <i>I</i> )	<i>I</i> > 2 $\sigma$ ( <i>I</i> )
<i>R</i> <sub>1</sub> ( <i>R</i> <sub>1</sub> all data)	0.0431 (0.0484)	0.0651 (0.0733)	0.0380 (0.0395)	0.0357 (0.0387)
<i>wR</i> <sub>2</sub> ( <i>wR</i> <sub>2</sub> all data)	0.0828 (0.0848)	0.1641 (0.1711)	0.0937 (0.0947)	0.0896 (0.0936)
Goodness of fit	1.239	1.081	1.095	1.161
CCDC deposition	925641	925643	925642	925640

**Scheme 2** Possible pathways used in the Jahng methodology and competing products. Reagents: (i) KO<sup>t</sup>Bu; (ii) NH<sub>4</sub>OAc, HOAc.

The electronic absorption spectra of degassed MeCN solutions of ligands **5**, **9** and **10** exhibited intense absorptions in the UV region arising from  $\pi^* \leftarrow \pi$  or  $\pi^* \leftarrow n$  transitions. Ligands **5**, **9** and **10** are emissive at 298 K in degassed MeCN. Excitation at *ca.* 280 nm leads to an emission at 342 nm for **5**, 458 nm for **9** and 461 nm for **10**.

Yellow blocks of **9** grew when an Et<sub>2</sub>O solution of the compound was left to evaporate slowly at room temperature. Fig. 1 shows the structure of **9**. The bpy unit adopts the expected *trans*-conformation. While the nitro group containing N4 lies within 1° of the plane of the ring to which it is bonded, that containing N3 is twisted 7.7° out of the corresponding ring plane. Despite this, the bond parameters for the two NO<sub>2</sub> groups indicate similar degrees of  $\pi$ -delocalization across the C<sub>arene</sub>-NO<sub>2</sub> units. The four rings in **9** are mutually twisted; the

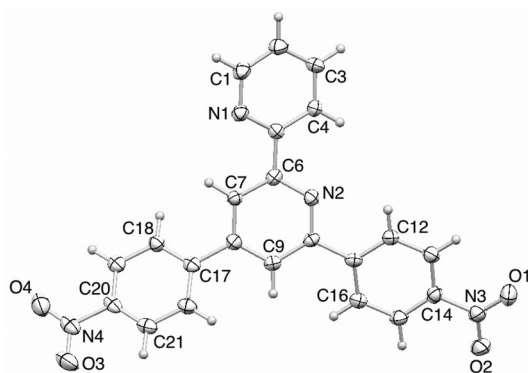


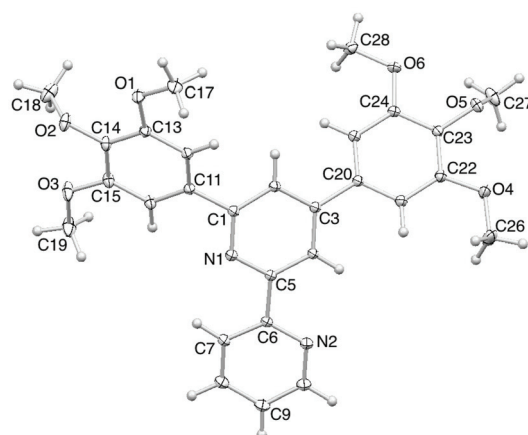
**Fig. 1** Structure of **9** (ellipsoids plotted at 40% probability). Selected bond distances and angles: N1–C1 = 1.335(8), N1–C5 = 1.348(7), N2–C10 = 1.338(7), N2–C6 = 1.339(7), C14–N3 = 1.464(8), C20–N4 = 1.477(8), N3–O1 = 1.228(8), N4–O3 = 1.207(8), N4–O4 = 1.217(8) Å; C1–N1–C5 = 117.5(5), C10–N2–C6 = 119.8(5), O2–N3–O1 = 122.5(6), O2–N3–C14 = 117.9(6), O1–N3–C14 = 119.6(6), O3–N4–O4 = 125.1(6), O3–N4–C20 = 118.3(6), O4–N4–C20 = 116.6(6)°.

angles between the rings containing atoms N1/N2, N2/C14 and N2/C20 are 12.8, 15.8 and 38.0°. The conformation of the ligand is intimately associated with the molecular packing. Pairs of pyridine and phenyl rings are slipped with respect to one another and do not engage in efficient face-to-face  $\pi$ -stacking. Two types of interactions appear to compensate for this: C–H $\cdots$ O<sub>nitro</sub> and face-to-face NO<sub>2</sub> $\cdots$  $\pi$  contacts.

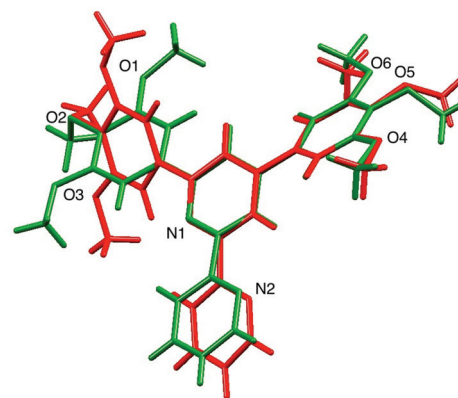
Polymorphic colourless prisms or needles of **10** grew when an Et<sub>2</sub>O or CH<sub>2</sub>Cl<sub>2</sub>–Et<sub>2</sub>O solution, respectively, of the compound was left to stand. Prisms of **10a** and needles of **10b** crystallize in the triclinic and monoclinic space groups  $P\bar{1}$  and  $P2_1/c$ , respectively. Fig. 2a shows the structure of **10a**, and an overlay of the molecular structures of the two polymorphs is shown in Fig. 2b; the same numbering scheme is used for both polymorphs. In terms of bond distances and angles, the structures differ little. In both **10a** and **10b**, the C<sub>arene</sub>–O bonds are shorter than the C<sub>methyl</sub>–O bonds, consistent with extension of the arene  $\pi$ -system onto the O atoms. The degree of deviation from planarity of the bpy domain in the two polymorphs differs (angle between ring planes = 14.8° in **10a** and 6.0° in **10b**). The most significant difference between **10a** and **10b** lies in the relative orientations of the 3,4,5-trimethoxyphenyl substituents. With respect to the pyridine ring containing atom N1, the phenyl rings are twisted 38.8 and 33.9° in **10a**, and 31.5 and 14.6° in **10b**. In each polymorph, the three methoxy substituents are arranged with the 3- and 5-substituted OMe groups lying approximately in the plane of the phenyl ring while the 4-OMe unit lies approximately orthogonal to it.

### Synthesis, mass spectrometric and NMR spectroscopic characterization of complexes

The complexes [Ir(ppy)<sub>2</sub>(N<sup>^</sup>N)][PF<sub>6</sub>] in which L = **1–12** (Scheme 1) were synthesized by treating [Ir(ppy)<sub>2</sub>( $\mu$ -Cl)]<sub>2</sub><sup>22,23</sup> with L followed by anion exchange (Scheme 3). The electro-spray mass spectrum of each product exhibited a peak



(a)

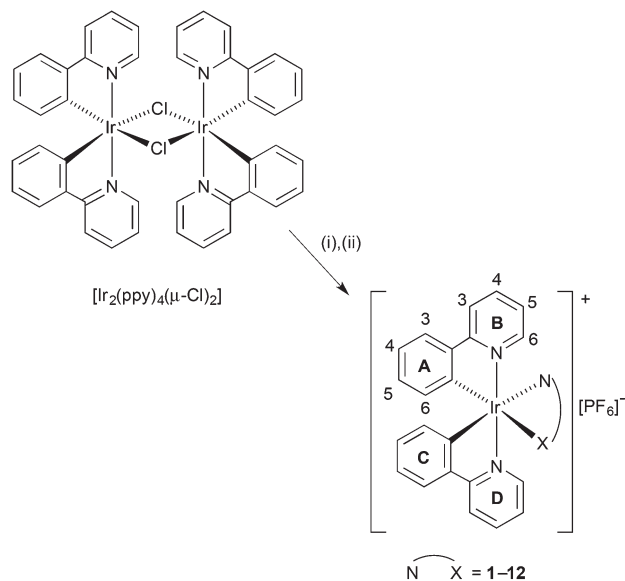


(b)

**Fig. 2** (a) Structure of **10a** (ellipsoids plotted at 40% probability). Selected bond distances: N1–C1 = 1.3531(8), N1–C5 = 1.3473(8), N2–C6 = 1.3496(9), N2–C10 = 1.3489(9), C13–O1 = 1.3645(8), C14–O2 = 1.3695(8), C15–O3 = 1.3620(8), C17–O1 = 1.4260(9), C18–O2 = 1.4310(10), C19–O3 = 1.4272(10), C22–O4 = 1.3666(8), C23–O5 = 1.3711(8), C24–O6 = 1.3604(8), C26–O4 = 1.4209(10), C27–O5 = 1.4249(9), C28–O6 = 1.4291(9) Å. (b) Overlay of the polymorphs **10a** (red) and **10b** (green).

envelope corresponding to the [M – PF<sub>6</sub>]<sup>+</sup> ion with an isotope pattern consistent with that calculated.

The <sup>1</sup>H and <sup>13</sup>C NMR spectra of the complexes were recorded in CD<sub>2</sub>Cl<sub>2</sub> and were assigned with the help of COSY, DEPT, NOESY, HMBC and HMQC methods and representative variable temperature experiments. The NMR spectroscopic signatures of [Ir(ppy)<sub>2</sub>(N<sup>^</sup>N)][PF<sub>6</sub>] for L = **1–11** confirmed that each ligand L acts as an N,N'-chelate; ligand **12** is an N,O-donor. Structural data (see below) confirmed that the O-atom of **12** lies *trans* to the C-donor of a [ppy]<sup>–</sup> ligand as shown in Scheme 3. In the parent complex [Ir(ppy)<sub>2</sub>(bpy)]<sup>+</sup>, the two [ppy]<sup>–</sup> ligands are equivalent but in each of [Ir(ppy)<sub>2</sub>(N<sup>^</sup>N)]<sup>+</sup> for L = **1–11**, the presence of the 6- or 4,6-substituents desymmetrizes the complex and the two pyridine rings and the two cyclometallated rings of the [ppy]<sup>–</sup> ligands are inequivalent. The <sup>1</sup>H NMR spectrum of [Ir(ppy)<sub>2</sub>(**3**)]<sup>+</sup>[PF<sub>6</sub>]<sup>–</sup> is shown in Fig. 3a. Signals for protons in rings A and C are well separated in the spectrum, but the distinction between resonances for protons



**Scheme 3** Synthesis of  $[\text{Ir}(\text{ppy})_2(\text{N}^{\text{A}}\text{N})][\text{PF}_6]$ . Conditions: (i) 2 equivalents of L, MeOH, 120 °C in a microwave reactor; (ii)  $\text{NH}_4\text{PF}_6$ . See Scheme 1 for L.

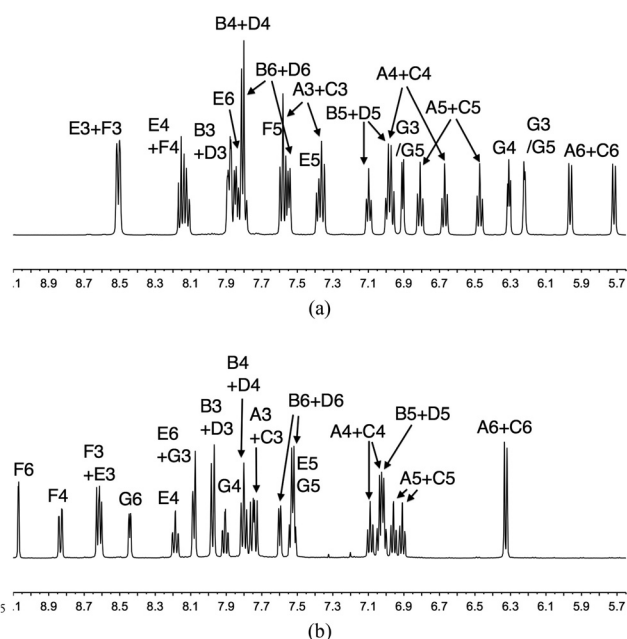


**Fig. 3** 500 MHz  $^1\text{H}$  NMR spectra of (a)  $[\text{Ir}(\text{ppy})_2(\mathbf{3})][\text{PF}_6]$  and (b)  $[\text{Ir}(\text{ppy})_2(\mathbf{11})][\text{PF}_6]$ . See Schemes 1 and 3 for ring and atom labelling. Scales are in  $\delta/\text{ppm}$ .

in pyridine rings B and D is less clear. This observation is typical for  $^1\text{H}$  spectra of all complexes  $[\text{Ir}(\text{ppy})_2(\text{N}^{\text{A}}\text{N})][\text{PF}_6]$  for  $L = 1\text{-}10$  and in related iridium(III) complexes.<sup>36,37</sup> In  $[\text{Ir}(\text{ppy})_2(\mathbf{11})][\text{PF}_6]$ , the environments of cyclometallated rings A and C are more similar (Fig. 3b) than in  $[\text{Ir}(\text{ppy})_2(\text{N}^{\text{A}}\text{N})][\text{PF}_6]$  with  $L = 1\text{-}10$ . This can be rationalized in terms of the substitution pattern in pyridine ring F. In  $[\text{Ir}(\text{ppy})_2(\text{N}^{\text{A}}\text{N})][\text{PF}_6]$  with  $L = 1\text{-}10$ , the 6-substituent lies over ring C (see structural discussions below), whereas in  $[\text{Ir}(\text{ppy})_2(\mathbf{11})][\text{PF}_6]$ , the 5-substituent is not so intimately associated with the coordination

sphere. This has been confirmed in the single crystal structure of  $[\text{Ru}(\text{bpy})_2(\mathbf{11})][\text{PF}_6]_2$ .<sup>38</sup>

The chirality of the tris-chelate  $[\text{Ir}(\text{ppy})_2(\text{N}^{\text{A}}\text{N})]^+$  cations has an influence only on the  $^1\text{H}$  NMR spectrum of  $[\text{Ir}(\text{ppy})_2(\mathbf{6})][\text{PF}_6]$ , in which the three  $\text{CH}_2$  groups of the butyl substituent in **6** are rendered diastereotopic. Signals for  $\text{H}^{\text{d}}$  (closest  $\text{CH}_2$  to the chiral iridium(III) centre) appear as two multiplets at  $\delta$  2.62 and 2.44 ppm, while for  $\text{H}^{\text{c}}$  and  $\text{H}^{\text{b}}$ , pairs of signals at  $\delta$  1.21 and 0.95 ppm, and at  $\delta$  0.73 and 0.63 ppm, respectively, are observed.

In the  $^1\text{H}$  and  $^{13}\text{C}$  NMR spectra of  $[\text{Ir}(\text{ppy})_2(\text{N}^{\text{A}}\text{N})][\text{PF}_6]$  with  $L = 2, 3, 4, 6, 11$  and **12**, all signals are sharp and well resolved. For the remaining complexes, dynamic behaviour causes broadening of some signals. In the spectrum of  $[\text{Ir}(\text{ppy})_2(\mathbf{1})][\text{PF}_6]$ , the signal at  $\delta$  3.01 ppm arising from the *N*-methyl group is broad (FWHM = 110 Hz) at 295 K. Signals for  $\text{H}^{\text{D}3}$  and  $\text{H}^{\text{D}6}$  are significantly broadened, while that assigned to  $\text{H}^{\text{G}5}$  has an approximate line width (FWHM) of 650 Hz. The ring labels are defined such that the pyrrole ring G lies over the  $[\text{ppy}]^-$  ligand containing rings C and D. Bearing in mind the solid-state structure described below, the broadened signals in the solution  $^1\text{H}$  NMR spectrum are consistent with hindered rotation of the *N*-methyl group. Proton  $\text{H}^{\text{G}5}$  is adjacent to, and  $\text{H}^{\text{D}6}$  lies below, the *N*-methyl substituent and both experience the effects of the changing proton environments as the methyl group rotates.

In the room temperature  $^1\text{H}$  NMR spectrum of  $[\text{Ir}(\text{ppy})_2(\mathbf{5})][\text{PF}_6]$ , signals for the 3-tolyl group of **5** are broadened; the signals for  $\text{H}^{\text{G}4}$  and  $\text{H}^{\text{G}5}$  appear as a broadened doublet and triplet, respectively, while a broad signal centred around  $\delta$  6.3 ppm (FWHM  $\approx$  100 Hz) is assigned to the coalescence of  $\text{H}^{\text{G}2}$  and  $\text{H}^{\text{G}6}$  (Fig. 4a). The  $^{13}\text{C}$  NMR signals for  $\text{C}^{\text{G}2}$  and  $\text{C}^{\text{G}6}$  ( $\delta$  128.6 and 124.9 ppm) were assigned on the basis of HMBC cross peaks to  $\text{H}^{\text{Me}}$  and  $\text{H}^{\text{G}4}$ , and to  $\text{H}^{\text{G}4}$ , respectively, as no HMQC cross peaks to the broad proton signal shown in Fig. 4a were observed. The dynamic behaviour of  $[\text{Ir}(\text{ppy})_2(\mathbf{8})]^+$  is

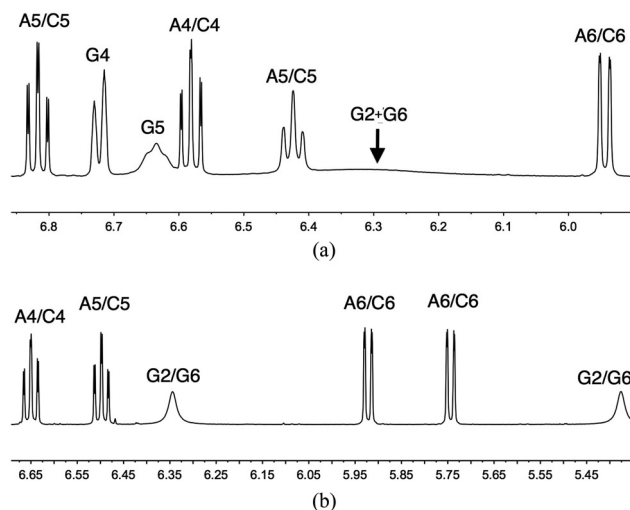


**Fig. 4** Parts of the room temperature 500 MHz  $^1\text{H}$  NMR spectra of  $\text{CD}_2\text{Cl}_2$  solutions of (a)  $[\text{Ir}(\text{ppy})_2(\mathbf{5})][\text{PF}_6]$  and (b)  $[\text{Ir}(\text{ppy})_2(\mathbf{10})][\text{PF}_6]$ .

similar to that of  $[\text{Ir}(\text{ppy})_2(\mathbf{5})]^+$ ; signals for phenyl ring G protons  $\text{H}^{\text{G4}}$ ,  $\text{H}^{\text{G3}}$  and  $\text{H}^{\text{G2}}$  in  $[\text{Ir}(\text{ppy})_2(\mathbf{8})][\text{PF}_6]$  appear as a triplet, broadened triplet and broad signal (FWHM  $\approx 30$  Hz), respectively at 295 K. In contrast to the hindered rotation of ring G on the NMR timescale, the 4-substituted phenyl ring H (Scheme 1) undergoes fast rotation. The fluxional behaviour of  $[\text{Ir}(\text{ppy})_2(\mathbf{8})]^+$  is reminiscent of that reported for  $[\text{Ir}(\text{ppy})_2(\text{N}^{\wedge}\text{N})]^+$  where L = 4-(3,5-dibromophenyl)-6-phenyl-2,2'-bipyridine.<sup>36</sup> The pendant pyridyl ring in **7** also undergoes hindered rotation at 295 K in a  $\text{CD}_2\text{Cl}_2$  solution of  $[\text{Ir}(\text{ppy})_2(\mathbf{7})][\text{PF}_6]$ . A broadened doublet at  $\delta$  8.01 ppm with a reduced coupling constant of  $\approx 5$  Hz is assigned to  $\text{H}^{\text{G2}}$  (Scheme 1). This doublet shows a COSY cross peak to a broad signal centred at  $\delta$  6.47 ppm and the latter is assigned to the coalescence of signals for  $\text{H}^{\text{G3}}$  and  $\text{H}^{\text{G5}}$ . The proton signals at  $\delta$  8.01 and 6.47 ppm correlate (HMQC) with  $^{13}\text{C}$  NMR resonances at 149.2 and 122.6 ppm, consistent with the higher frequency signal arising from the  $^{13}\text{C}$  nucleus adjacent to the nitrogen atom.

Fig. 4b shows part of the solution  $^1\text{H}$  NMR spectrum of  $[\text{Ir}(\text{ppy})_2(\mathbf{10})][\text{PF}_6]$  at 295 K. The inequivalence and shielding of  $\text{H}^{\text{G2}}$  and  $\text{H}^{\text{G6}}$  (Scheme 1) are consistent with the solid-state structure described below. The broadening of the signals indicates some degree of dynamic behaviour. In contrast, ring H (Scheme 1) undergoes fast rotation on the NMR timescale with the *ortho*-protons giving rise to a sharp singlet at  $\delta$  7.06 ppm.

As a representative study, we recorded the  $^1\text{H}$  NMR spectrum of  $[\text{Ir}(\text{ppy})_2(\mathbf{9})][\text{PF}_6]$  at temperatures over the range 295 to 210 K. Most signals are essentially independent of temperature, but Fig. 5 illustrates that a broad signal ( $\delta$  7.60 ppm) assigned to  $\text{H}^{\text{G3}}$  at 295 K collapses on cooling and gives rise to two signals at  $\delta$  7.42 and 7.74 ppm. In the 295 K spectrum, a very broad signal (FWHM  $\approx 150$  Hz) centred *ca.*  $\delta$  6.8 ppm can be discerned. On cooling, this sharpens to give a doublet ( $\delta$  6.22 ppm) at 210 K (Fig. 5); its partner appears at  $\delta$  7.37 ppm at 210 K. These signals are assigned to  $\text{H}^{\text{G2}}$  and  $\text{H}^{\text{G6}}$ , and the significant difference in their chemical shifts is consistent with the two protons facing into and away from the ring

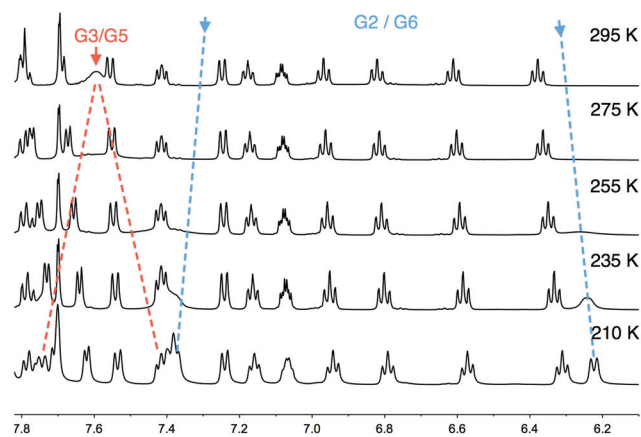


**Fig. 5** Part of the variable temperature 500 MHz  $^1\text{H}$  NMR spectrum of a  $\text{CD}_2\text{Cl}_2$  solution of  $[\text{Ir}(\text{ppy})_2(\mathbf{9})][\text{PF}_6]$  showing coalescence of pairs of *ortho*- and *meta*-protons in 4-nitrophenyl ring G.

current of phenyl ring C over which ring G is stacked in the static structure. The solid-state structure of  $[\text{Ir}(\text{ppy})_2(\mathbf{9})][\text{PF}_6]$  is detailed below.

### Single crystal structures

Single crystals of  $2\{[\text{Ir}(\text{ppy})_2(\mathbf{1})][\text{PF}_6]\} \cdot \text{C}_6\text{H}_5\text{Me}$  were grown by layering a chloroform solution of  $[\text{Ir}(\text{ppy})_2(\mathbf{1})][\text{PF}_6]$  with toluene. Fig. 6 shows the structure of the  $[\text{Ir}(\text{ppy})_2(\mathbf{1})]^+$  cation in the asymmetric unit. The iridium(III) ion is octahedrally sited with the pyridine rings of the two  $[\text{ppy}]^-$  ligands in the anticipated *trans*-arrangement. The cation is chiral and since the compound crystallizes in the orthorhombic *Pbcn* space group, both the  $\Delta$ - (Fig. 6a) and  $\Lambda$ -enantiomers are present in

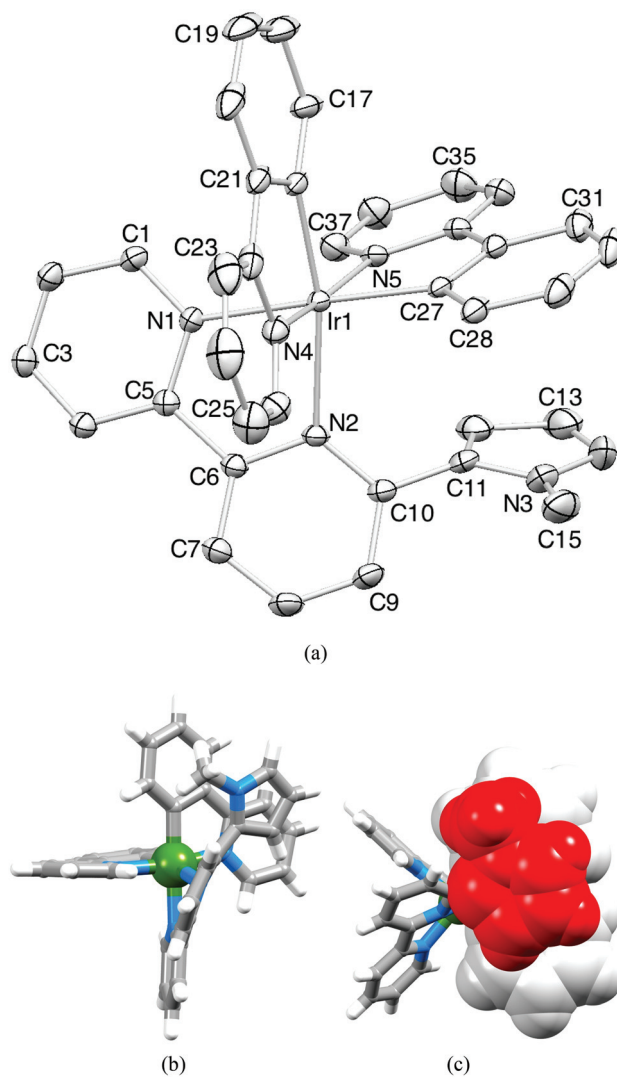


**Fig. 6** (a) Structure of the  $\Delta$ - $[\text{Ir}(\text{ppy})_2(\mathbf{1})]^+$  cation in  $2\{[\text{Ir}(\text{ppy})_2(\mathbf{1})][\text{PF}_6]\} \cdot \text{C}_6\text{H}_5\text{Me}$  (H atoms omitted; ellipsoids plotted at 30% probability). Selected bond parameters: Ir1–N1 = 2.144(4), Ir1–N2 = 2.193(4), Ir1–N4 = 2.037(5), Ir1–N5 = 2.034(4), Ir1–C16 = 1.990(5), Ir1–C27 = 2.012(5), N3–C15 = 1.442(11) Å; N1–Ir1–N2 = 75.55(16), N5–Ir1–C27 = 80.4(2), N4–Ir1–C16 = 80.6(2), N4–Ir1–N5 = 170.13(17), C27–Ir1–N1 = 178.17(17), C16–Ir1–N2 = 167.6(2), C27–Ir1–N2 = 102.64(17)°. (b) Projection of the cation to illustrate the twisting of ligand **1**. (c) Stacking of the *N*-pyrrole ring over one of the two  $[\text{ppy}]^-$  ligands.

the unit cell. The presence of the *N*-methyl pyrrole ring causes distortion as can be seen from the four obtuse bond angles listed in the caption to Fig. 6a. Whereas the two [ppy]<sup>−</sup> ligands are essentially planar, the backbone of **1** is noticeably twisted (Fig. 6b); the angles between the least squares planes of the rings containing N1/N2 and N2/N3 are 21.7 and 53.4°. The latter allows the pyrrole ring to stack over one [ppy]<sup>−</sup> ligand (Fig. 6c, distance from centroid of pyrrole ring to plane of [ppy]<sup>−</sup> = 3.4 Å), but the angle between the planes of aromatic domains is 19.3°. The *N*-methyl substituent appears to sterically hinder the face-to-face  $\pi$ -interaction, and is responsible for the distorted octahedral geometry of atom Ir1. However, we note that in [Cu(**1**)<sub>2</sub>][PF<sub>6</sub>] (pseudo-tetrahedral copper(i) ion), the two ligands in the cation achieve an efficient intramolecular aryl embrace with a face-to-face  $\pi$ -interaction between the pyrrolyl unit of one ligand and the central pyridine ring of the other.<sup>18</sup> It is not, therefore, the presence of the *N*-methyl group *per se* that prevents the interaction in [Ir(ppy)<sub>2</sub>(**1**)]<sup>+</sup> being more efficient, rather a combination of this and the angular restriction that the octahedral coordination sphere imposes. The toluene molecule is disordered over a special position, as is one of the two half [PF<sub>6</sub>]<sup>−</sup> anions present in the asymmetric unit. Pairs of cations embrace one another through a face-to-face interaction between the [ppy]<sup>−</sup> ligands containing N1 and N4<sup>i</sup> (symmetry code *i* = *x*, 1 − *y*, −<sup>1</sup>/<sub>2</sub> + *z*) but the relative orientations of the rings does not allow for the most efficient of packing interactions. CH...F contacts make a major contribution to the overall packing interactions.

Slow evaporation of CH<sub>2</sub>Cl<sub>2</sub> solutions of [Ir(ppy)<sub>2</sub>(**9**)][PF<sub>6</sub>] or [Ir(ppy)<sub>2</sub>(**10**)][PF<sub>6</sub>] produced single crystals of X-ray quality. The former crystallized as 2{[Ir(ppy)<sub>2</sub>(**9**)][PF<sub>6</sub>]}·CH<sub>2</sub>Cl<sub>2</sub>·2H<sub>2</sub>O and structural determination confirmed the expected octahedral coordination environment of the iridium(III) ion. The racemic complex crystallizes in the centrosymmetric *P*<sub>1</sub> space group; the structure of the  $\Delta$ -enantiomer is shown in Fig. 7. [Ir(ppy)<sub>2</sub>(**10**)][PF<sub>6</sub>] crystallizes in the centrosymmetric *P*<sub>2</sub><sub>1</sub>/*n* space group and enantiomers of the octahedral cation are present in the lattice; the structure of the  $\Lambda$ -[Ir(ppy)<sub>2</sub>(**10**)]<sup>+</sup> cation is depicted in Fig. 8. Bond lengths and angles in both complexes are unexceptional and selected data are given in the captions to Fig. 7 and 8. In [Ir(ppy)<sub>2</sub>(**9**)]<sup>+</sup>, each nitro group lies in the plane of the phenyl ring to which it is bonded consistent with electron delocalization. The plane of the phenyl ring containing C17 is twisted 32.0° with respect to the pyridine ring with N2; the plane of 6-substituted ring (containing C11) deviates from the plane of the pyridine ring containing N2 by 63.4°. In [Ir(ppy)<sub>2</sub>(**10**)]<sup>+</sup>, the corresponding twist angles are 28.3 and 70.5°. The greater twisting of the 6-substituent is consistent with it lying over one of [ppy]<sup>−</sup> ligands – that containing N5 in [Ir(ppy)<sub>2</sub>(**9**)]<sup>+</sup> or N4 in [Ir(ppy)<sub>2</sub>(**10**)]<sup>+</sup>. The face-to-face  $\pi$ -interaction that results is more efficient in [Ir(ppy)<sub>2</sub>(**10**)]<sup>+</sup> than in [Ir(ppy)<sub>2</sub>(**9**)]<sup>+</sup> (Fig. 9), the angle between the least squares planes of the phenyl and [ppy]<sup>−</sup> unit being 5.5 and 18.2°, respectively.

In [Ir(ppy)<sub>2</sub>(**10**)][PF<sub>6</sub>], the [PF<sub>6</sub>]<sup>−</sup> anion is ordered. Packing interactions involve extensive CH...F and CH...O contacts, in

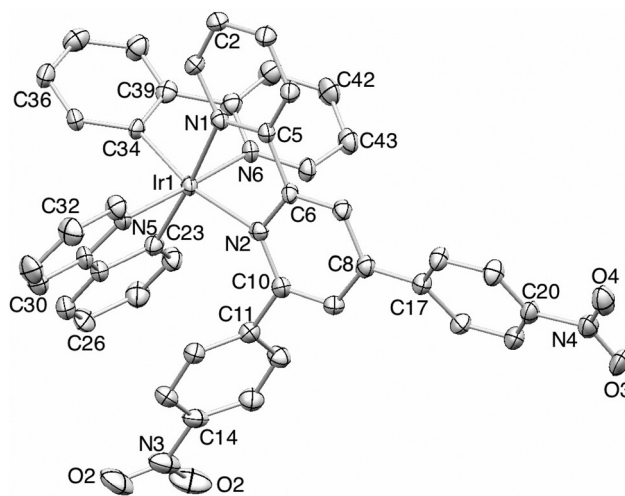


**Fig. 7** Structure of the  $\Delta$ -[Ir(ppy)<sub>2</sub>(**9**)]<sup>+</sup> cation in racemic 2{[Ir(ppy)<sub>2</sub>(**9**)][PF<sub>6</sub>]}·CH<sub>2</sub>Cl<sub>2</sub>·2H<sub>2</sub>O (H atoms omitted; ellipsoids plotted at 30% probability). Selected bond parameters: Ir1–N1 = 2.144(4), Ir1–N2 = 2.201(4), Ir1–N5 = 2.046(5), Ir1–N6 = 2.055(5), Ir1–C23 = 2.014(5), Ir1–C34 = 1.993(4), C14–N3 = 1.465(7), N3–O1 = 1.196(9), N3–O2 = 1.240(10), C20–N4 = 1.469(6), N4–O3 = 1.226(7), N4–O4 = 1.235(7) Å; N1–Ir1–N2 = 75.98(14), C34–Ir1–N6 = 80.6(2), C23–Ir1–N5 = 80.2(2), N5–Ir1–N6 = 174.53(15), O1–N3–O2 = 123.1(6), O3–N4–O4 = 124.0(5)°.

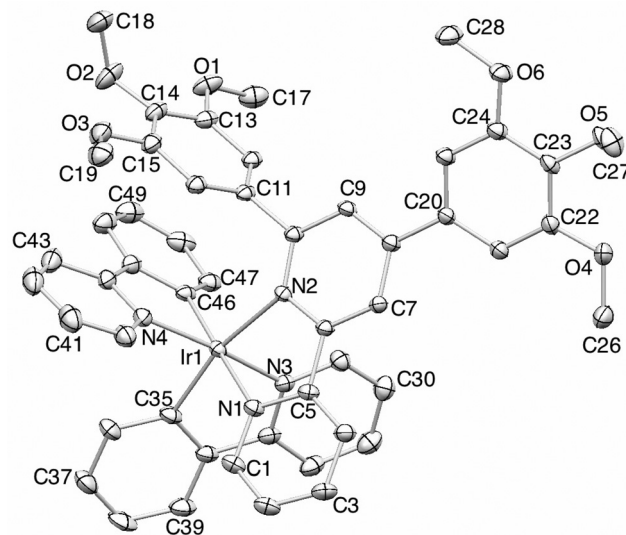


**Fig. 8** Structure of the  $\Lambda$ -[Ir(ppy)<sub>2</sub>(**10**)]<sup>+</sup> cation in racemic [Ir(ppy)<sub>2</sub>(**10**)][PF<sub>6</sub>] (H atoms omitted; ellipsoids plotted at 30% probability). Selected bond parameters: Ir1–N1 = 2.134(3), Ir1–N2 = 2.204(3), Ir1–N3 = 2.053(3), Ir1–N4 = 2.047(3), Ir1–C35 = 2.012(4), Ir1–C46 = 2.012(4), C13–O1 = 1.361(5), C17–O1 = 1.424(6), C14–O2 = 1.371(5), C18–O2 = 1.412(6), C15–O3 = 1.363(5), C19–O3 = 1.427(6), C22–O4 = 1.355(5), C26–O4 = 1.422(6), C2–O5 = 1.373(4), C27–O5 = 1.420(5), C24–O6 = 1.367(5), C28–O6 = 1.426(6) Å; N1–Ir1–N2 = 75.04(11), C35–Ir1–N3 = 81.01(16), C46–Ir1–N4 = 80.21(16), N4–Ir1–N3 = 171.26(13)°.

addition to face-to-face  $\pi$ -stacking between symmetry related pairs of trimethoxyphenyl domains (interplane distance = 3.55 Å and inter-centroid separation = 3.75 Å between rings containing C20 and C20<sup>i</sup>, symmetry code *i* = 1 − *x*, −*y*, −*z*). The [PF<sub>6</sub>]<sup>−</sup> anion in 2{[Ir(ppy)<sub>2</sub>(**9**)][PF<sub>6</sub>]}·CH<sub>2</sub>Cl<sub>2</sub>·2H<sub>2</sub>O is ordered;

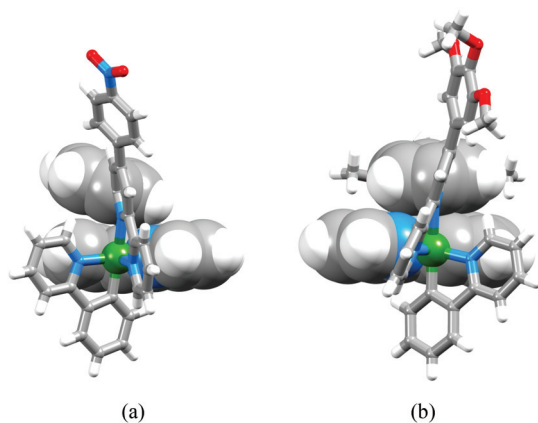


Fig. 9 Intra-cation face-to-face  $\pi$ -stacking in (a)  $[\text{Ir}(\text{ppy})_2(\mathbf{9})]^+$  and (b)  $[\text{Ir}(\text{ppy})_2(\mathbf{10})]^+$ .

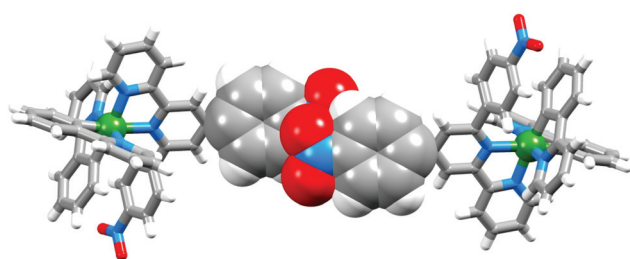


Fig. 10 Stacking interactions between centrosymmetric pairs of 4-nitrophenyl substituents in  $2\{[\text{Ir}(\text{ppy})_2(\mathbf{9})][\text{PF}_6]\} \cdot \text{CH}_2\text{Cl}_2 \cdot 2\text{H}_2\text{O}$ .

the structure contains disordered solvates modelled as half-occupancy  $\text{CH}_2\text{Cl}_2$  and four half occupancy water molecules. Packing interactions between cations and anions involve short  $\text{CH}\cdots\text{F}$  and  $\text{CH}\cdots\text{O}$  contacts. Intermolecular interactions between nitro-substituents have been studied in detail and a variety of modes are present in organic nitro-derivatives; where hydrogen bonds are absent, zig-zag  $\text{NO}\cdots\text{N}$  or  $\text{O}\cdots\text{O}$  contacts have been observed.<sup>39</sup> In  $2\{[\text{Ir}(\text{ppy})_2(\mathbf{9})][\text{PF}_6]\} \cdot \text{CH}_2\text{Cl}_2 \cdot 2\text{H}_2\text{O}$ , the 4-nitrophenyl group (containing N4) engages in a stacked interaction with a symmetry related substituent (containing N4<sup>i</sup>,  $i = 2 - x, -1 - y, 1 - z$ ) in an adjacent cation (Fig. 10); the interplane separation is 2.90 Å, and  $\text{N4}\cdots\text{O3}^i = 2.97(1)$  Å.

The chelation of ligand **12** through an N,O-donor set was confirmed with a single crystal structure determination of  $2\{[\text{Ir}(\text{ppy})_2(\mathbf{12})][\text{PF}_6]\} \cdot \text{MeOH} \cdot 2\text{H}_2\text{O}$ . The complex crystallizes in the centrosymmetric space group  $P2_1/c$  with both enantiomers of the octahedral tris(chelate) in the unit cell. Fig. 11a shows the structure of the  $\Delta$ - $[\text{Ir}(\text{ppy})_2(\mathbf{12})]^+$  cation. The *trans*-arrangement of the N-donors of the two  $[\text{ppy}]^-$  ligands is expected and consistent with the other structures reported in this work. Bond parameters for the coordination environment are typical. The O1–C6 bond distance of 1.253(6) Å indicates retention of C–O  $\pi$ -character upon coordination of the ketone unit; conjugation extends along the alkene and dimethyl amino backbone with the greatest deviation of any of atoms C6, C7, C8, N2, C9

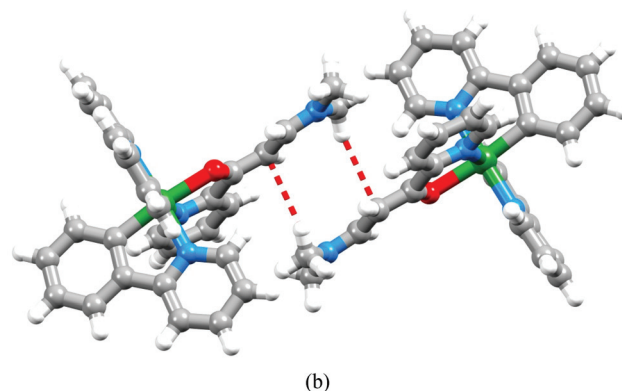
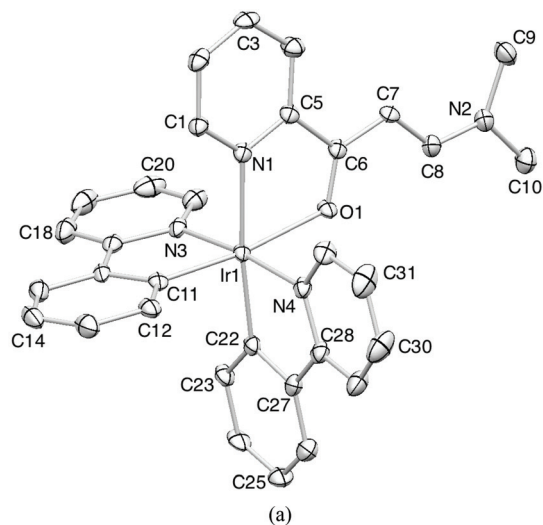


Fig. 11 (a) Structure of the  $\Delta$ - $[\text{Ir}(\text{ppy})_2(\mathbf{12})]^+$  cation in racemic  $2\{[\text{Ir}(\text{ppy})_2(\mathbf{12})][\text{PF}_6]\} \cdot \text{MeOH} \cdot 2\text{H}_2\text{O}$  (H atoms omitted; ellipsoids plotted at 30% probability). Selected bond parameters: Ir1–N1 = 2.137(4), Ir1–O1 = 2.173(3), Ir1–N3 = 2.021(4), Ir1–N4 = 2.033(4), Ir1–C11 = 1.987(5), Ir1–C22 = 2.002(5), C7–C8 = 1.385(7), N2–C8 = 1.314(6), N2–C9 = 1.449(7), N2–C10 = 1.463(7), O1–C6 = 1.253(6) Å; N1–Ir1–O1 = 75.40(13), C22–Ir1–N4 = 80.92(18), C11–Ir1–N3 = 80.72(19), N3–Ir1–N4 = 173.92(16), C8–N2–C9 = 122.3(4), C8–N2–C10 = 120.2(5), C9–N2–C10 = 117.5(4)°. (b) Packing of pairs of centrosymmetric cations through  $\text{NMe}_2\cdots\text{alkene}$  contacts.

and C10 from a least squares plane being 0.03 Å. The  $[\text{PF}_6]^-$  anion is ordered, but solvent molecules are disordered and have been modelled as a half-occupancy MeOH molecule and two half-occupancy water molecules. Ignoring the disordered solvent molecules, packing interactions involve  $\text{CH}\cdots\text{F}$  and  $\text{CH}\cdots\text{O}$  contacts. Pairs of cations related by an inversion centre embrace one another through  $\text{NMe}_2\cdots\text{alkene}$  interactions (Fig. 11b). The shortest  $\text{H}\cdots\text{C}_{\text{alkene}}$  separations are 2.88 Å.

### Electrochemistry

The complexes are all redox active. Oxidation and reduction potentials measured using cyclic voltammetry are summarized in Table 2. The reversible oxidation wave is assigned to an iridium-centred process, in keeping with theoretical calculations carried out on related complexes.<sup>40</sup> Values of  $E_{1/2}^{\text{ox}}$  in Table 2 compare to 0.81 V for the complex  $[\text{Ir}(\text{ppy})_2(6\text{-Phbpy})][\text{PF}_6]$  where 6-Phbpy = 6-phenyl-2,2'-bipyridine.<sup>41</sup> The structural influence

**Table 2** Cyclic voltammetric data for  $[\text{Ir}(\text{ppy})_2(\text{N}^{\wedge}\text{N})][\text{PF}_6]$  with  $L = 1-12$  with respect to  $\text{Fc}/\text{Fc}^+$ ; MeCN solutions with  $[\text{tBu}_4\text{N}][\text{PF}_6]$  as supporting electrolyte and scan rate of  $0.1 \text{ V s}^{-1}$ . Processes are reversible unless otherwise stated; qr = quasi-reversible, irr = irreversible

$[\text{Ir}(\text{ppy})_2(\text{N}^{\wedge}\text{N})]^+$	$E_{1/2}^{\text{ox}}/\text{V}$	$E_{1/2}^{\text{red}}/\text{V}$	$E_{\text{gap}}/\text{eV}$
$[\text{Ir}(\text{ppy})_2(1)]^+$	0.80	-1.80, -2.47, -2.60 <sup>qr</sup>	2.18
$[\text{Ir}(\text{ppy})_2(2)]^+$	0.92	-1.77, -2.45, -2.62	2.27
$[\text{Ir}(\text{ppy})_2(3)]^+$	0.88	-1.78, -2.45, -2.58 <sup>qr</sup>	2.24
$[\text{Ir}(\text{ppy})_2(4)]^+$	0.85	-1.77, -2.43, -2.58 <sup>qr</sup>	2.19
$[\text{Ir}(\text{ppy})_2(5)]^+$	0.85	-1.80 <sup>qr</sup> , -2.24, -2.46 <sup>qr</sup>	2.31
$[\text{Ir}(\text{ppy})_2(6)]^+$	0.96	-1.85 <sup>qr</sup> , -2.32, -2.57	2.38
$[\text{Ir}(\text{ppy})_2(7)]^+$	0.91	-1.74 <sup>qr</sup> , -2.16, -2.44, -2.56	2.26
$[\text{Ir}(\text{ppy})_2(8)]^+$	0.86	-1.76 <sup>qr</sup> , -2.38, -2.58 <sup>qr</sup>	2.25
$[\text{Ir}(\text{ppy})_2(9)]^+$	0.95	-1.30, -1.51, -1.64	1.81
$[\text{Ir}(\text{ppy})_2(10)]^+$	0.85	-1.78, -2.39, -2.58 <sup>qr</sup>	2.22
$[\text{Ir}(\text{ppy})_2(11)]^+$	0.90	-1.33, -1.80	1.86
$[\text{Ir}(\text{ppy})_2(12)]^+$	0.67	-1.58, -2.08, -2.54	1.89

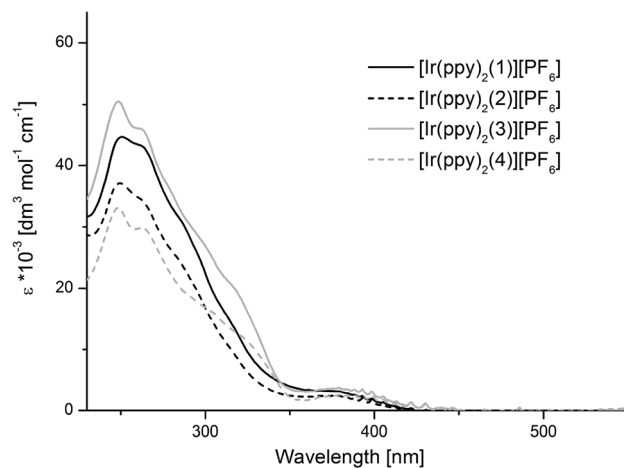
of the 6-substituent on the electronic structure of the complex is clear from the variation in  $E_{1/2}^{\text{ox}}$  which does not follow a simple pattern based on electron withdrawing or releasing nature of the substituents. Replacing the bpy-ligand by the N,O-donor in  $[\text{Ir}(\text{ppy})_2(12)][\text{PF}_6]$  results in a more easily oxidized metal centre. Each of  $[\text{Ir}(\text{ppy})_2(\text{N}^{\wedge}\text{N})][\text{PF}_6]$  with  $L = 1-8$  and  $10$  exhibits a reversible or quasi-reversible ligand-based reduction process close to the  $-1.75 \text{ V}$  observed for  $[\text{Ir}(\text{ppy})_2(6\text{-Phbpy})][\text{PF}_6]$ .<sup>41</sup>  $[\text{Ir}(\text{ppy})_2(9)][\text{PF}_6]$  exhibits three reversible processes at lower potentials (Table 2) consistent with reduction processes associated with the nitrophenyl substituents.

### Photophysical properties

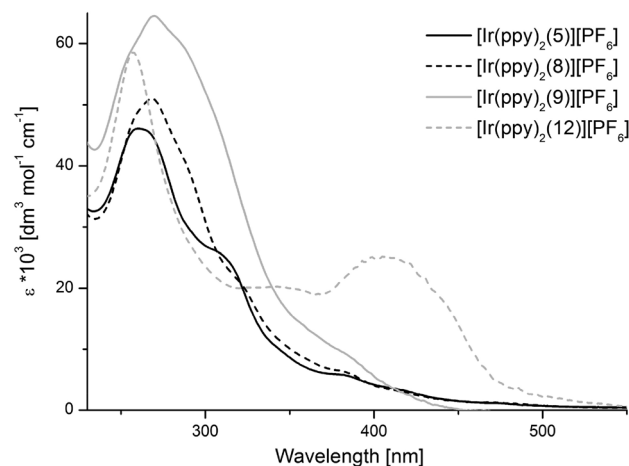
Table 3 lists the absorption maxima in the UVVIS spectra of  $[\text{Ir}(\text{ppy})_2(\text{N}^{\wedge}\text{N})][\text{PF}_6]$  with  $L = 1-12$ . Representative spectra are shown in Fig. 12. All the complexes are orange with the exception of  $[\text{Ir}(\text{ppy})_2(11)][\text{PF}_6]$  and  $[\text{Ir}(\text{ppy})_2(12)][\text{PF}_6]$  which are red and dark red, respectively. Fig. 12a shows that the absorption spectra of  $[\text{Ir}(\text{ppy})_2(\text{N}^{\wedge}\text{N})][\text{PF}_6]$  with  $L = 1-4$  are similar, with broad, intense absorptions in the UV region and a tail into the

**Table 3** Electronic absorption band maxima for MeCN (degassed) solutions of  $[\text{Ir}(\text{ppy})_2(\text{N}^{\wedge}\text{N})][\text{PF}_6]$  with  $L = 1-12$

Cation	$\lambda_{\text{max}}/\text{nm}$ ( $\epsilon_{\text{max}}/10^3 \text{ dm}^3 \text{ mol}^{-1} \text{ cm}^{-1}$ )
$[\text{Ir}(\text{ppy})_2(1)]^+$	252 (44.5), 264 (43.3), 287sh (30.4), 375 (3.4)
$[\text{Ir}(\text{ppy})_2(2)]^+$	250 (37.0), 264 (34.0), 286sh (23.8), 377 (3.7)
$[\text{Ir}(\text{ppy})_2(3)]^+$	248 (50.8), 264 (46.2), 296sh (28.5), 378 (3.7)
$[\text{Ir}(\text{ppy})_2(4)]^+$	249 (32.9), 264 (30.0), 305sh (16.0), 324sh (11.3), 384 (2.4)
$[\text{Ir}(\text{ppy})_2(5)]^+$	261 (40.6), 310 (21.5), 380 (3.7)
$[\text{Ir}(\text{ppy})_2(6)]^+$	256 (49.2), 306 (25.8), 380 (4.7)
$[\text{Ir}(\text{ppy})_2(7)]^+$	257 (57.6), 310 (31.0), 379 (8.9)
$[\text{Ir}(\text{ppy})_2(8)]^+$	268 (51.2), 320sh (21.1), 383 (6.1)
$[\text{Ir}(\text{ppy})_2(9)]^+$	253sh (58.0), 270 (64.5), 383 (9.5)
$[\text{Ir}(\text{ppy})_2(10)]^+$	257 (45.9), 270 (46.2), 291sh (40.2), 391 (7.3)
$[\text{Ir}(\text{ppy})_2(11)]^+$	262 (53.8), 310 (27.8), 382 (5.3)
$[\text{Ir}(\text{ppy})_2(12)]^+$	257 (58.7), 410 (25.2)



(a)



(b)

**Fig. 12** Electronic absorption spectra of  $[\text{Ir}(\text{ppy})_2(\text{N}^{\wedge}\text{N})][\text{PF}_6]$  in degassed MeCN: (a)  $L = 1-4$ ; (b)  $L = 5, 8, 9$  and  $12$ .

visible region. A similar spectrum is observed for  $[\text{Ir}(\text{ppy})_2(5)][\text{PF}_6]$  (Fig. 12b) and  $[\text{Ir}(\text{ppy})_2(7)][\text{PF}_6]$ . The introduction of additional aromatic substituents on going to  $[\text{Ir}(\text{ppy})_2(8)][\text{PF}_6]$ ,  $[\text{Ir}(\text{ppy})_2(9)][\text{PF}_6]$  and  $[\text{Ir}(\text{ppy})_2(10)][\text{PF}_6]$  is accompanied by the expected increase in intensity of the ligand-based absorptions (Fig. 12b). On going to  $[\text{Ir}(\text{ppy})_2(12)][\text{PF}_6]$  (Fig. 12b), a relatively intense absorption at 410 nm is observed which we assign to an MLCT band.

With the exception of  $[\text{Ir}(\text{ppy})_2(12)][\text{PF}_6]$  which contains an N,O-chelating ligand, all the complexes are orange emitters in degassed MeCN solution at room temperature. The excitation and emission wavelengths are given in Table 4; the excitation spectrum of each complex was recorded to confirm the origin of the emission. For the complexes containing 6-substituted bpy ligands  $1-5$  and  $11$ ,  $\lambda_{\text{max}}^{\text{em}}$  lies in the range 601–608 nm. Each of these ligands contains an aromatic substituent. These emission wavelengths are red-shifted with respect to those of the 585 nm for  $[\text{Ir}(\text{ppy})_2(\text{bpy})][\text{PF}_6]$ <sup>40</sup> and 595 nm for  $[\text{Ir}(\text{ppy})_2(6\text{-Phbpy})][\text{PF}_6]$  (6-Phbpy = 6-phenyl-2,2'-bipyridine).<sup>41</sup> A blue-shift in the emission (to 575 nm) is observed on going

**Table 4** Room temperature emission data for MeCN (degassed,  $1.0 \times 10^{-5}$  mol  $\text{dm}^{-3}$ ) solutions of  $[\text{Ir}(\text{ppy})_2(\text{N}^{\wedge}\text{N})][\text{PF}_6]$  with  $L = 1-11$ 

$[\text{Ir}(\text{ppy})_2(\text{N}^{\wedge}\text{N})]^+$	$\lambda_{\text{exc}}/\text{nm}$	$\lambda_{\text{max}}^{\text{em}}/\text{nm}$	Quantum yield <sup>a</sup>
$[\text{Ir}(\text{ppy})_2(\mathbf{1})]^+$	257	608	<0.01
$[\text{Ir}(\text{ppy})_2(\mathbf{2})]^+$	260	601	<0.01
$[\text{Ir}(\text{ppy})_2(\mathbf{3})]^+$	259	606	<0.01
$[\text{Ir}(\text{ppy})_2(\mathbf{4})]^+$	259	606	<0.01
$[\text{Ir}(\text{ppy})_2(\mathbf{5})]^+$	261	606	<0.01
$[\text{Ir}(\text{ppy})_2(\mathbf{6})]^+$	257	575	<0.01
$[\text{Ir}(\text{ppy})_2(\mathbf{7})]^+$	262	605	0.04
$[\text{Ir}(\text{ppy})_2(\mathbf{8})]^+$	265	611	<0.01
$[\text{Ir}(\text{ppy})_2(\mathbf{9})]^+$	362	578	<0.01
$[\text{Ir}(\text{ppy})_2(\mathbf{10})]^+$	257	607	<0.01
$[\text{Ir}(\text{ppy})_2(\mathbf{11})]^+$	259	601	<0.01

<sup>a</sup> PL and QY measurements were made on different instruments, see Experimental section.

from the latter to  $[\text{Ir}(\text{ppy})_2(\mathbf{6})]^+$  which contains a 6-*n*-butyl substituent. For complexes containing the 4,6-disubstituted ligands **8–10**, the effect of the substituents is most noticeable for **9** where  $\lambda_{\text{max}}^{\text{em}}$  is blue-shifted by *ca.* 30 nm upon the introduction of the electron withdrawing nitro-groups (Table 4). With the exception of  $[\text{Ir}(\text{ppy})_2(\mathbf{7})][\text{PF}_6]$  which contains the pendant pyridyl substituent, quantum yields are below the detectable limit of the instrument (Table 4).

### Photoluminescence in thin films and ionic liquid medium

Five of the complexes were selected for an investigation of their photoluminescence in thin films (5% in weight of the complex in PMMA) and in ionic liquid (1-butyl-3-methylimidazolium hexafluoridophosphate) with a molar ratio iTMC : IL 4 : 1 (device configuration). Two families were chosen:  $[\text{Ir}(\text{ppy})_2(\text{N}^{\wedge}\text{N})][\text{PF}_6]$  in which  $\text{N}^{\wedge}\text{N} = 1-3$  (aromatic heterocyclic substituent in the 6-position of the bpy ligand) and  $[\text{Ir}(\text{ppy})_2(\text{N}^{\wedge}\text{N})][\text{PF}_6]$  with  $\text{N}^{\wedge}\text{N} = 8$  and **10** (4,6-diaryl-substituted bpy ligands). The diluted thin-film photoluminescence spectra exhibited maxima at 565, 564 and 563 nm with quantum yields of 34, 42 and 41% for  $\text{N}^{\wedge}\text{N} = 1, 2$  and **3**, respectively ( $\lambda_{\text{exc}} = 314$  nm). Each emission is blue shifted by *ca.* 40 nm with respect to the solution maximum (Table 4) but, as in solution, a change in the heteroatom in the pendant substituent in the  $\text{N}^{\wedge}\text{N}$  ligand has minimal effect upon the emission. In an ionic liquid medium (Fig. 13a), the emissions are again similar for the three complexes ( $\lambda_{\text{max}}^{\text{em}} = 595, 595$  and 594 for the complexes with  $\text{N}^{\wedge}\text{N} = 1, 2$  and **3**, respectively) and are red-shifted with respect to the diluted thin film emission maxima; quantum yields are 11, 14 and 14%, respectively. Thus, the quantum yields are greatly enhanced on going from fluid solution (Table 4) to diluted thin film and even in the device configuration with only a small amount of ionic liquid present.

The emission maxima of  $[\text{Ir}(\text{ppy})_2(\mathbf{8})][\text{PF}_6]$  and  $[\text{Ir}(\text{ppy})_2(\mathbf{10})][\text{PF}_6]$  in ionic liquid are both 600 nm (Fig. 13b), and show only a small blue shift compared to the solution data in Table 4. Quantum yields are again significantly enhanced (15% for  $[\text{Ir}(\text{ppy})_2(\mathbf{8})][\text{PF}_6]$  and 19% for  $[\text{Ir}(\text{ppy})_2(\mathbf{10})][\text{PF}_6]$ ).

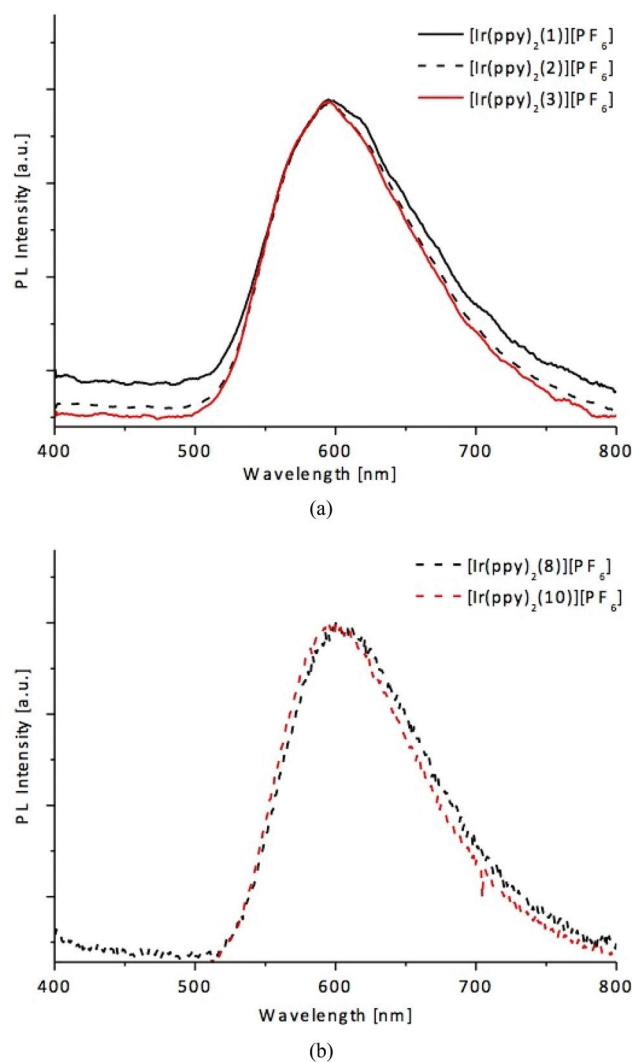


**Fig. 13** Photoluminescence spectra for  $[\text{Ir}(\text{ppy})_2(\text{N}^{\wedge}\text{N})][\text{PF}_6]/[\text{BMIM}][\text{PF}_6]$  (4 : 1) in the solid state: (a)  $\text{N}^{\wedge}\text{N} = 1-3$ , (b)  $\text{N}^{\wedge}\text{N} = 8$  and **10**.

### Device performances

In view of the promising photoluminescence efficiency data for the thin films, LEC devices were prepared using the complexes  $[\text{Ir}(\text{ppy})_2(\text{N}^{\wedge}\text{N})][\text{PF}_6]$  with  $\text{N}^{\wedge}\text{N} = 1, 2, 3, 8$  and **10** according to the procedure described in the Experimental section. Devices consisted of a 100 nm emitting layer, comprising the iTMC-complex and the ionic liquid  $[\text{BMIM}][\text{PF}_6]$  in a molar ratio of iTMC : IL 4 : 1, sandwiched between an ITO/PEDOT:PSS (100 nm) anode and a thermally evaporated aluminum cathode (70 nm). PEDOT:PSS was used to smooth the ITO surface, increasing the yield and reproducibility of working devices, whereas the ionic liquid was employed to facilitate charge injection into the devices, thereby reducing the turn-on time. The LECs using complexes  $[\text{Ir}(\text{ppy})_2(\text{N}^{\wedge}\text{N})][\text{PF}_6]$  with  $\text{N}^{\wedge}\text{N} = 1, 2$  or **3** were driven under a dc voltage of 4 V, whereas those using complexes  $[\text{Ir}(\text{ppy})_2(\text{N}^{\wedge}\text{N})][\text{PF}_6]$  with  $\text{N}^{\wedge}\text{N} = 8$  and **10** were operated using a pulsed current driving method. The

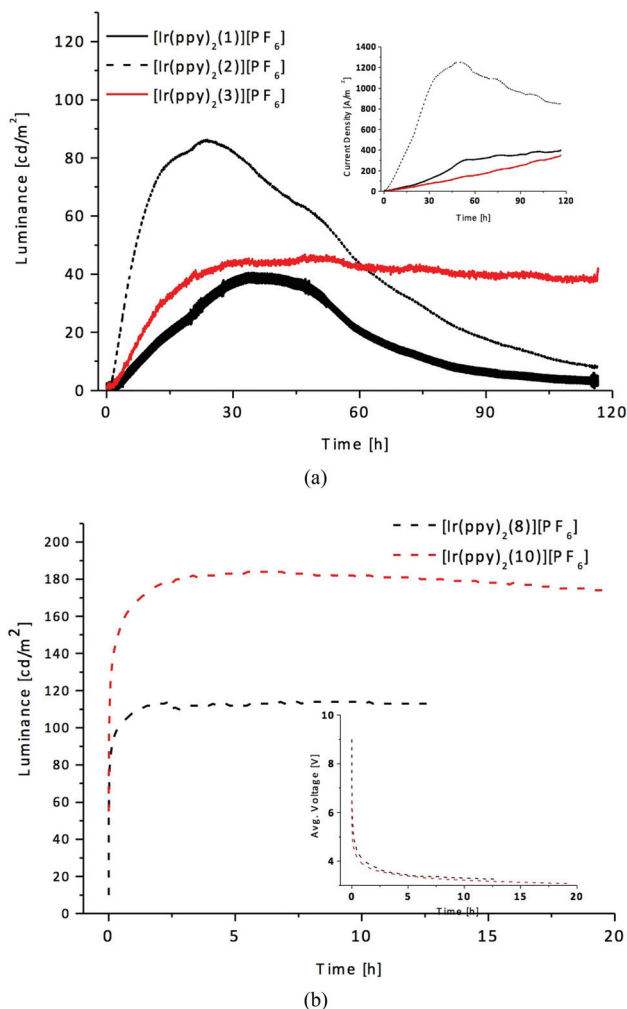


**Fig. 14** (a) Luminance and current density (inset) versus time for ITO/PEDOT:PSS/[Ir(ppy)<sub>2</sub>(N<sup>N</sup>)]PF<sub>6</sub>/IL(4:1)/Al LEC: (a) N<sup>N</sup> = 1–3 with devices biased by 4V DC; (b) N<sup>N</sup> = 8 and 10 with devices biased by a pulsed current of 50 A m<sup>-2</sup> (1000 Hz, 50% duty cycle, block wave).

luminance and current/average voltage characteristics versus operation time are shown in Fig. 14.

Very fast turn of the luminance is observed accompanied by a rapid decrease of the average voltage applied. This is evidence of the particular operation mechanism of the LECs.<sup>42,43</sup> The ions present in the light-emitting film migrate to the respective electrodes under the influence of the applied bias, and as a result decrease the barrier for electron injection. Under current driving this leads to a strong reduction of the voltage to sustain the pre-set current density. The light emission turns-on very rapidly as well, even though the maximum emission is only observed after a few hours. When compared with voltage driving the turn-on of luminance is much faster. Once the maximum luminance is obtained it only gradually decreases with time leading to quite good lifetimes. More importantly the efficiency is also much more stable with time and remains almost constant over the lifetime of the devices. A summary of the most important device parameters is given in Table 5.

**Table 5** Performance of LEC devices, either (a) driven using a constant voltage mode (4V) for [Ir(ppy)<sub>2</sub>(N<sup>N</sup>)]PF<sub>6</sub> with N<sup>N</sup> = 1, 2 or 3 or (b) using a pulsed current mode (average current density 50 A m<sup>-2</sup>, 1000 Hz, 50% duty cycle, block wave) for [Ir(ppy)<sub>2</sub>(N<sup>N</sup>)]PF<sub>6</sub> with N<sup>N</sup> = 8 or 10

[Ir(ppy) <sub>2</sub> (N <sup>N</sup> )] <sup>+</sup>	t <sub>on</sub> /h	L <sub>max</sub> /cd m <sup>-2</sup>	t <sub>1/2</sub> /h	Efficacy/cd A <sup>-1</sup>	Power efficiency/lm W <sup>-1</sup>	EQE/%
[Ir(ppy) <sub>2</sub> (1)] <sup>+</sup>	33	41	61	1.5	0.4	0.3
[Ir(ppy) <sub>2</sub> (2)] <sup>+</sup>	24	86	58	0.5	0.3	0.2
[Ir(ppy) <sub>2</sub> (3)] <sup>+</sup>	28	46	335 <sup>a</sup>	2.7	1.5	0.9
[Ir(ppy) <sub>2</sub> (8)] <sup>+</sup>	2.4	114	125 <sup>a</sup>	2.4	1.2	1.2
[Ir(ppy) <sub>2</sub> (10)] <sup>+</sup>	3.3	182	130 <sup>a</sup>	3.7	1.8	1.7

<sup>a</sup> Value from extrapolation.

The device data show clearly that the bulky ligands used for [Ir(ppy)<sub>2</sub>(8)]PF<sub>6</sub> and [Ir(ppy)<sub>2</sub>(10)]PF<sub>6</sub> are beneficial for the operation of LECs. In view of the PL quantum yields observed in thin film configuration and assuming a light outcoupling efficiency of 20% for these planar devices, maximum EQEs for the LECs using complex [Ir(ppy)<sub>2</sub>(8)]PF<sub>6</sub> and [Ir(ppy)<sub>2</sub>(10)]PF<sub>6</sub> of 3 and 3.8% are expected. Hence, the observed values are quite good, especially taking into account that the exciton to photon conversion efficiency is decreased under influence of an electric field.

## Conclusions

We have described the preparation and characterization of a series of [Ir(ppy)<sub>2</sub>(N<sup>N</sup>)]PF<sub>6</sub> complexes in which each N<sup>N</sup> ligand contains a bpy-core and is functionalized in the 6- or 5-positions. The substituents are structurally and electronically very varied, but most contain an aromatic ring that is designed to permit the formation of an intra-cation  $\pi$ -stacking interaction with one of the [ppy]<sup>-</sup> domains. Single crystal X-ray diffraction studies of [Ir(ppy)<sub>2</sub>(N<sup>N</sup>)]PF<sub>6</sub> containing 1, 9, 10 and 12 confirm the presence of this interaction, although the presence of the *N*-methyl substituent in 1 results in a significantly distorted octahedral coordination environment for the iridium(III) centre. In solution, <sup>1</sup>H NMR spectroscopy has been used to investigate the dynamic behaviour of the complexes. The preparation and characterization of a representative [Ir(ppy)<sub>2</sub>(N<sup>O</sup>)]<sup>+</sup> complex (N<sup>O</sup> = 12) has also been described. In degassed MeCN and at room temperature, the [Ir(ppy)<sub>2</sub>(N<sup>N</sup>)]PF<sub>6</sub> complexes are all orange emitters with  $\lambda_{\text{max}}^{\text{em}}$  in the range 575 to 608 nm; quantum yields are very low. [Ir(ppy)<sub>2</sub>(12)]PF<sub>6</sub> is non-emissive. The variation in the oxidation potential of the iridium ion compared to literature data for [Ir(ppy)<sub>2</sub>(6-Phbpy)]PF<sub>6</sub> suggests that the structural influence of the 6-substituent on the electronic structure of the complex is the dominant factor; there is no simple trend that can be associated with electron-withdrawing or releasing nature of the substituents on the N<sup>N</sup> domain. The complexes with the bulky N<sup>N</sup> ligands 8 and 10 lead to very interesting LECs that show quite good performances. In view of the limited photoluminescence efficiency, very good external quantum efficiencies are

obtained indicating a good balance between electron and holes.

## Acknowledgements

We thank the European Research Council (Advanced Grant 267816 LiLo), the Swiss National Science Foundation, and the University of Basel for financial support, the Spanish Ministry of Economy and Competitiveness (MINECO) (MAT2011-24594, CTQ2009-08790 and Consolider-Ingenio CSD2007-00010), the Generalitat Valenciana (PROMETEO/2012/053), and the European Union (CELLO, STRP 248043; <https://www.cello-project.eu/>) for financial support. A.P. also acknowledges MINECO for an FPI grant. Nik Hostettler is thanked for recording low temperature NMR spectra.

## Notes and references

- Q. B. Pei, G. Yu, C. Zhang, Y. Yang and A. J. Heeger, *Science*, 1995, **269**, 1086.
- H. J. Bolink, F. Monti, G. Accorsi and N. Armaroli, *Angew. Chem., Int. Ed.*, 2012, **51**, 8178.
- R. D. Costa, E. Ortí and H. J. Bolink, *Pure Appl. Chem.*, 2011, **83**, 2115.
- F. Dumar, D. Bertin and D. Gigmes, *Int. J. Nanotechnol.*, 2012, **9**, 377.
- T. Hu, L. He, L. Duan and Y. Qiu, *J. Mater. Chem.*, 2012, **22**, 4206.
- See for example: J. D. Slinker, A. A. Gorodetsky, M. S. Lowry, J. Wang, S. Parker, R. Rohl, S. Bernhard and G. G. Malliaras, *J. Am. Chem. Soc.*, 2004, **126**, 2763.
- C. Dragonetti, L. Falciola, P. Mussini, S. Righetto, D. Roberto, R. Ugo, A. Valore, F. De Angelis, S. Fantacci, A. Sgamellotti, M. Ramon and M. Muccini, *Inorg. Chem.*, 2007, **46**, 8533 and references therein.
- M. Lepeltier, T. K.-M. Lee, K. K.-W. Lo, L. Toupet, H. Le Bozec and V. Guerschais, *Eur. J. Inorg. Chem.*, 2005, 110.
- M. S. Lowry, W. R. Hudson, R. A. Pascal Jr. and S. Bernhard, *J. Am. Chem. Soc.*, 2004, **126**, 14129.
- S. Fantacci and F. De Angelis, *Coord. Chem. Rev.*, 2011, **255**, 2704.
- F. Neve, A. Crispini, S. Campagna and S. Serroni, *Inorg. Chem.*, 1999, **38**, 2250.
- H. J. Bolink, E. Coronado, R. D. Costa, E. Ortí, M. Sessolo, S. Graber, K. Doyle, M. Neuburger, C. E. Housecroft and E. C. Constable, *Adv. Mater.*, 2008, **20**, 3910.
- R. D. Costa, E. Ortí, H. J. Bolink, S. Graber, C. E. Housecroft, M. Neuburger, S. Schaffner and E. C. Constable, *Chem. Commun.*, 2009, 2029.
- R. D. Costa, E. Ortí, H. J. Bolink, S. Graber, S. Schaffner, M. Neuburger, C. E. Housecroft and E. C. Constable, *Adv. Funct. Mater.*, 2009, **19**, 3456.
- R. D. Costa, E. Ortí, H. J. Bolink, S. Graber, C. E. Housecroft and E. C. Constable, *Adv. Funct. Mater.*, 2010, **20**, 1511.
- R. D. Costa, E. Ortí, H. J. Bolink, S. Graber, C. E. Housecroft and E. C. Constable, *J. Am. Chem. Soc.*, 2010, **132**, 5978.
- R. D. Costa, E. Ortí, H. J. Bolink, S. Graber, C. E. Housecroft and E. C. Constable, *Chem. Commun.*, 2011, 3207.
- B. Bozic-Weber, E. C. Constable, C. E. Housecroft, P. Kopecky, M. Neuburger and J. A. Zampese, *Dalton Trans.*, 2011, **40**, 12584.
- M. M. Abdel-Khalik and M. H. Elnagdi, *Synth. Commun.*, 2002, **32**, 159.
- S. Bindal, D. Kumar, N. Damodara, S. Bhatiya and A. K. Chakraborti, *Synthesis*, 2011, 1930.
- T. Kuffmann, J. Koenig and A. Woltermann, *Chem. Ber.*, 1976, **109**, 3864.
- S. Sprouse, K. A. King, P. J. Spellane and R. J. Watts, *J. Am. Chem. Soc.*, 1984, **106**, 6647.
- M. Nonoyama, *Bull. Chem. Soc. Jpn.*, 1974, **47**, 767.
- See for example: E. C. Constable, A. M. W. Cargill Thompson, J. Cherryman and T. Liddiment, *Inorg. Chim. Acta*, 1995, **235**, 165; D. A. Beauchamp and S. J. Loeb, *Supramol. Chem.*, 2005, **17**, 617.
- G. W. V. Cave and C. L. Raston, *J. Chem. Soc., Perkin Trans. 1*, 2001, 3285.
- Stoe & Cie, *IPDS software v 1.26*, Stoe & Cie, Darmstadt, Germany, 1996.
- G. M. Sheldrick, *Acta Crystallogr., Sect. A: Fundam. Crystallogr.*, 2008, **64**, 112.
- APEX2, version 2 User Manual, M86-E01078*, Bruker Analytical X-ray Systems, Inc., Madison, WI, 2006.
- A. Altomare, G. Casciarano, G. Giacovazzo, A. Guagliardi, M. C. Burla, G. Polidori and M. Camalli, *J. Appl. Crystallogr.*, 1994, **27**, 435.
- P. W. Betteridge, J. R. Carruthers, R. I. Cooper, K. Prout and D. J. Watkin, *J. Appl. Crystallogr.*, 2003, **36**, 1487.
- I. J. Bruno, J. C. Cole, P. R. Edgington, M. K. Kessler, C. F. Macrae, P. McCabe, J. Pearson and R. Taylor, *Acta Crystallogr., Sect. B: Struct. Sci.*, 2002, **58**, 389.
- C. F. Macrae, I. J. Bruno, J. A. Chisholm, P. R. Edgington, P. McCabe, E. Pidcock, L. Rodriguez-Monge, R. Taylor, J. van de Streek and P. A. Wood, *J. Appl. Crystallogr.*, 2008, **41**, 466.
- F. Kröhnke, *Synthesis*, 1976, 1.
- Y. Jahng and J. G. Park, *Inorg. Chim. Acta*, 1998, **267**, 265.
- Y. Jahng and J. G. Park, *Bull. Korean Chem. Soc.*, 1998, **19**, 436.
- A. M. Bünzli, H. J. Bolink, E. C. Constable, C. E. Housecroft, M. Neuburger, A. Pertegás and J. A. Zampese, *Eur. J. Inorg. Chem.*, 2012, 3780.
- E. Baranoff, H. J. Bolink, E. C. Constable, M. Delgado, D. Häussinger, C. E. Housecroft, M. K. Nazeeruddin, M. Neuburger, E. Ortí, G. E. Schneider, D. Tordera, R. M. Walliser and J. A. Zampese, *Dalton Trans.*, 2013, **42**, 1073.

- 38 E. C. Constable, C. E. Housecroft, P. Kopecky, C. J. Martin, I. A. Wright and J. A. Zampese, *Polyhedron*, 2013, DOI: 10.1016/j.poly.2013.01.059.
- 39 I. Mossakowska and G. M. Wójcik, *J. Mol. Struct.*, 2010, **967**, 119.
- 40 R. D. Costa, E. Ortí, D. Tordera, A. Pertegás, H. J. Bolink, S. Graber, C. E. Housecroft, L. Sachno, M. Neuburger and E. C. Constable, *Adv. Energy. Mater.*, 2011, **1**, 282.
- 41 R. D. Costa, E. Ortí, H. J. Bolink, S. Graber, C. E. Housecroft and E. C. Constable, *Adv. Funct. Mater.*, 2010, **20**, 1511.
- 42 M. Lenes, G. Garcia-Belmonte, D. Tordera, A. Pertegás, J. Bisquert and H. J. Bolink, *Adv. Funct. Mater.*, 2011, **21**, 1581.
- 43 D. Tordera, S. Meier, M. Lenes, R. D. Costa, E. Ortí, W. Sarfer and H. J. Bolink, *Adv. Mater.*, 2012, **24**, 854.